NACA TN 3095

NATIONAL ADVISORY COMMITTEE FOR AERONAUTICS

TECHNICAL NOTE 3095

THE AMES 10- BY 14-INCH SUPERSONIC WIND TUNNEL

By A. J. Eggers, Jr. and George J. Nothwang

Ames Aeronautical Laboratory
Moffett Field, Calif.

Washington
January 1954

1X

NATIONAL ADVISORY COMMITTEE FOR AERONAUTICS

TECHNICAL NOTE 3095

THE AMES 10- BY 14-INCH SUPERSONIC WIND TUNNEL

By A. J. Eggers, Jr. and George J. Nothwang

SUMMARY

The Ames 10- by 14-inch supersonic wind tunnel is described and pertinent features of the design and operation of the facility are included. The wind tunnel is capable of continuous operation at Mach numbers from 2.7 to 6.3 and Reynolds numbers from 1 million to 11 million per foot. Results of surveys of the test section show that the Mach number variation along the tunnel center line is less than ±1 percent at all Mach numbers, except at the nominal Mach number setting of 6.3 where the variation reaches ±2 percent. The corresponding variations in static pressure result in a buoyancy correction to the zero-lift foredrag of a typical test body of revolution of 3 percent or less at all test Mach numbers. The variation in stream angle along the tunnel center line is less than ±0.2° at all Mach numbers. Larger variations in stream static pressure and stream angle are encountered off the tunnel center line.

INTRODUCTION

The Ames 10- by 14-inch supersonic wind tunnel was designed to provide aerodynamic data on aircraft at speeds varying from supersonic to hypersonic. To aid in this design, experiments were undertaken in 1946 with a 1- by 1.4-inch nozzle which became the pilot nozzle for the wind tunnel. This nozzle was employed more recently to study aspects of condensation in supersonic wind tunnels and is described in detail in reference 1. The pilot nozzle was tested with a variety of diffuser shapes of the now well-known converging-diverging type, and the results of these tests dictated the shape of the diffuser employed in the 10- by 14-inch tunnel. Because of the small size of the equipment, it was not undertaken to determine an optimum effuser shape for this wind tunnel. Rather, it was assumed that an effuser which produces flow of the necessary uniformity in the test section could be obtained by analysis, in particular, with the method of characteristics.

With the results of this analysis and the experimental data obtained from the pilot nozzle, the 10- by 14-inch supersonic wind tunnel was designed to cover the Mach number range from about 3 to 6. Construction of the tunnel was completed in December 1949. Initial calibration of the tunnel revealed that condensation of air occurred in the test section at Mach numbers greater than about 4.4, and that the extent of this condensation was sufficient at test Mach numbers in excess of 5 to make it

impractical to obtain data under such conditions. For this reason, the experiments reported in reference 1 were undertaken, and the results of these experiments dictated the addition of a heater to the supply air system of the tunnel. With this addition, condensation-free flow can be obtained in the test section at Mach numbers up to 6.3.

The purpose of the present report is to describe the 10- by 14-inch supersonic wind tunnel and its operational characteristics over the nominal Mach number range from 2.7 to 6.3. Rather complete calibration data on characteristics of flow in the test section are presented and briefly discussed.

DESCRIPTION OF WIND TUNNEL

Nozzle and Drive Equipment

The Ames 10- by 14-inch supersonic wind tunnel is of the continuous-flow, closed-throat nonreturn type (see fig. 1). Air is supplied to the wind tunnel by centrifugal compressors at a maximum pressure of 6 atmospheres absolute. The absolute humidity of the air delivered to the tunnel is maintained at a value below 0.0001 pound of water per pound of air by passing the air from the compressors first through an aftercooler and then through a silica gel dryer. At test Mach numbers greater than 4.4, the air entering the wind tunnel is preheated by an electrical heater to eliminate condensation in the test section. A maximum stagnation temperature of about 400° F is obtainable at the nominal test Mach number of 6.3. Depending upon the Mach number, from 15 to 30 percent of the air passing into the diffuser of the wind tunnel is drawn off through the boundary-layer scoops located at the second throat (see fig. 1), while the remaining 70 to 85 percent of the air passes through the main diffuser. The air passing through the boundary-layer scoops is compressed by rotary vacuum pumps before being discharged to the atmosphere. These vacuum pumps develop a maximum compression ratio of 30:1. At Mach numbers of 4.2 and below, air passing through the main diffuser is exhausted directly to the atmosphere. At Mach numbers in excess of 4.2, air in the main diffuser is diverted through either one or two stages of centrifugal evacuators, developing a maximum compression ratio of 3:1 per stage, before being discharged to the atmosphere. These evacuators are, in fact, turbosuperchargers, and the turbine wheels are driven by excess air from the supply air compressors of the wind tunnel.

A view of the wind tunnel proper with one side wall removed is shown in figure 2. The 10-inch dimension corresponds to the width of the tunnel and is constant from the entrance of the effuser to the exit of the diffuser. The 14-inch dimension corresponds to the nominal depth of the test section. As is seen in figure 2, the tunnel proper is composed of an effuser, a test section, and converging-diverging diffuser, all of which will hereafter be referred to as the nozzle. The nozzle blocks are

symmetrical, rigid, built-up steel structures, and each is connected with wrist pins to jackscrews at the first and second throat. These screws are, in turn, supported by the nozzle side walls. By properly moving the jacks, it is clear that both the first throat and second throat may be opened or closed. The jacks at the first throat are connected through a chain drive to one common motor and the jacks at the second throat are connected to another common motor. With this arrangement, the nozzle passage always remains symmetrical when the nozzle blocks are moved. It is evident, of course, from the geometry of the nozzle, that closing the first throat will increase the ratio of test-section area to first-throat area and, hence, increase the Mach number of the flow in the test section; while closing the second throat decreases the ratio of second-throat area to test-section area and thereby decreases the Mach number of flow in this throat. Hence, once supersonic flow is established in the region between the first and second throats, the test-section Mach number may be varied by simply changing the first-throat area, while relatively high diffuser efficiency may be maintained by properly adjusting the second-throat area. It is implicit, of course, to the successful operation of this tunnel that essentially uniform flow be obtained in the test section over a wide range of high supersonic speeds using only one set of nozzle blocks. That this might be achieved was verified, as pointed out in the Introduction, by a characteristics analysis of the nozzle. The ordinates of the nozzle blocks are presented in table I.

The boundary-layer scoops are also apparent in figure 2, the entrances thereto being located at the second throat of the nozzle. Each scoop passage is bounded by the side walls, one nozzle block and a plate separating the passage from the main diffuser. This plate has its leading edge at the second throat and is attached to the nozzle block by (a) a hinge located about 4 feet downstream of this throat, and (b) a remotely controlled motor-actuated strut (see fig. 2) located midway between the hinge and the throat. Moving the strut then rotates the separating plate about its hinge and thus changes the entrance area to the scoop. In this manner the scoop may be adjusted to remove all the low-energy boundary-layer air on the blocks and thus stabilize flow in the diverging portion of the main diffuser over the test Mach number range.

Seals run the full length of the nozzle on each side of the nozzle blocks. These seals are of the inflatable rubber type, rectangular in cross section, and are made of heat-resistant rubber. They are pressurized to 100 pounds per square inch gage and contact the side walls to within about 1/8 inch of the inside surfaces of the nozzle blocks. The function of these seals is to prevent appreciable leakage into the nozzle air stream either from the atmosphere or adjacent regions within the nozzle.

Neither the steel side walls of the nozzle nor the steel side plates of the nozzle blocks are perfectly plane and parallel. Consequently, in order to prevent seizing between these parts, it was necessary to separate

them with bronze bearing pads. These pads are attached to the nozzle blocks as indicated in figure 2.

Auxiliary Equipment

Auxiliary equipment for the wind tunnel includes a center-of-curvature-type schlieren apparatus for observing flow about models, McLeod type manometers for measuring pressures on the surfaces of models, and a strain-gage balance with electronic follow-up system for measuring and recording forces and moments acting on models. Also available is an X-ray densitometer for determining local air densities in the flow about models.

A view of the schlieren apparatus is shown in figure 1. The light source, which is a water-cooled mercury-vapor lamp, is located at the center of curvature of the principal mirror in the system. This mirror is located immediately adjacent to one window of the side wall of the test section and is spherical with a 25-foot focal length. The knife, which may be placed in either the vertical or horizontal attitude, is located just to one side of the light source. The 50-foot distance from the knife and light source to the principal mirror is obtained by folding the light beam twice with the aid of optical flats. The image of the test section can be focused either on a ground glass screen or in a camera situated adjacent to this screen. The schlieren system is enclosed in a shroud which serves two functions: (a) It forms the support for all elements of the schlieren system, and (b) it prevents transient disturbances in the ambient air outside the wind tunnel from distorting the schlieren picture. The shroud is supported from above by four coil springs designed to isolate from the schlieren system high-frequency disturbances originating in the main building.

The McLeod manometers are mounted in a battery of 40 tubes, all of which are connected to a common sump. These manometers use mercury as a working fluid and are designed to give pressure measurements accurate within 1 percent over the range of pressures from 1 mm to 78 mm of mercury absolute. In general, only the closed leg of each manometer is exposed at the front of the board. The two reference tubes at the extreme ends of the board are the exceptions and are maintained at vacuum pressure. When equilibrium pressures have been established in all tubes and the sump raised, the front of the board may be photographed, yielding a picture not unlike that obtained from conventional U-tube manometer boards.

The strain-gage balance is of the conventional, external-to-model type, being designed to measure forces and moments on models sting supported from it. Lift gages are mounted from the balance beam while the rear of the beam bears on the drag gage. Both lift and pitching moment may be obtained from the lift gages by employing the proper electrical

connection. However, it has been found that greater sensitivity in moment measurements is obtained if moment gages are mounted directly on the sting. The electronic follow-up equipment consists simply of a photo-cell-type galvanometer and printer for each force or moment circuit. At the present time only lift, drag, and pitching moment have been measured simultaneously, although the follow-up system has elements for one additional force or moment component.

The X-ray densitometer has already been described in detail in reference 2, including its application to the 10- by 14-inch wind tunnel, and will not be discussed further here.

OPERATION OF THE WIND TUNNEL

Operation of the wind tunnel is, in practice, carried out from a control panel located adjacent to the nozzle (see fig. 1). In particular, nozzle-block and boundary-layer-scoop settings are controlled remotely from this panel. Likewise, all valves in the air lines to and from the tunnel may be remotely adjusted from here - the same applies to control of the supply air heater. The procedure for operating the wind tunnel is, then, essentially as follows: The nozzle blocks are set in the position to develop supersonic flow at a test Mach number of approximately 3.5. The appropriate valves in the supply air and exhaust lines of the wind tunnel are then opened and supersonic flow is established. After a particular test Mach number is set, model tests may be conducted, including, for example, the determination of the dependence of forces and moments on Reynolds number and angle of attack. As soon as these measurements are made, the tunnel Mach number is then changed to the next required value and the desired aerodynamic measurements are again made. This procedure may be repeated at as many as six Mach numbers over the range from 2.7 to 6.3 without ever shutting the wind tunnel down to change nozzle or model setting. Under normal circumstances, lift, drag, and pitching moment for a particular model may be determined for a range of angles of attack of 10° over this Mach number range in a period of approximately three hours. Pressure-distribution measurements over a comparable range of angles of attack and Mach numbers require a somewhat greater period, due to the time required for the McLeod manometers to reach equilibrium pressure.

SURVEY APPARATUS AND TECHNIQUES

Four rakes were used in the calibration of the 10- by 14-inch supersonic wind tunnel. The coordinate system used in designating points in the test section is illustrated in figure 3 and the notation is defined in the Appendix. A pitot-static rake, shown in figure 4, was used in preliminary tests to determine Mach number and Reynolds number ranges of the wind tunnel. This rake was also used to ascertain if the flow along

the tunnel center line of the test section was free from condensed air at Mach numbers above 4.4 (see ref. 1). The pertinent dimensions of this rake are shown in figure 4. The pitot-pressure needle was simply a stainless steel tube with the upstream end machined flat and perpendicular to the axis of the tube. The tube had an outside-to-inside diameter ratio of 1.5. Tests in the 10- by 14-inch tunnel showed no measurable effect of diameter ratio on pitot pressures for tubes having outside-to-inside diameter ratios from 1.5 to 10. The static-pressure probe had a 10° apex-angle cone followed by a cylinder. There were four orifices equally spaced around the circumference and located 16 diameters from the cone apex. This probe gave the most accurate results of those tested in reference 3. Additional tests in the 10- by 14-inch tunnel revealed no discernible effect of orifice location on the measured static pressure for probes having orifices located 16, 20, and 24 diameters from the cone apex. Static pressures measured with this needle are believed accurate to within ±2 percent of true static pressure.

The detailed pressure survey of the test region was made with the pitot-pressure rake shown in figure 5. This rake contained 15 pitot-pressure probes similar to that in the pitot-static rake. A static-pressure rake was also constructed (see fig. 6). This rake contained seven static-pressure needles like that in the pitot-static rake. The static-pressure rake afforded a check on the static pressures determined from the pitot-pressure survey and thus provided a check on the existence of condensed air within a 3-1/2-inch radius of the tunnel center line.[1]

Stream angles were measured with the rake shown in figure 7. The rake contained three cones with 20° apex angles. Each cone had two 0.031-inch-diameter orifices, 180° apart, located 1 inch from the apex. The cones could be rotated to measure stream angles in two planes 90° apart. The cones were calibrated at each test Mach number by inclining the rake at several angles of attack. It was found that the pressure differential between each pair of orifices varied linearly with angle of attack in the calibrated range of $\pm 2^{\circ}$. Local stream angles were determined from measured pressure differentials with the aid of the calibration curves and mechanically measured cone inclinations. The measurements are estimated to be accurate within $\pm 0.15^{\circ}$.

Reservoir pressures and pressures in the exhaust lines of the main diffuser and boundary-layer scoops were measured with Bourdon type

---

[1]A detailed static-pressure survey was not made because:

(a) Pitot pressure is more sensitive to Mach number in the range of the 10- by 14-inch wind tunnel (i.e., $dH'/dM > dp/dM$).

(b) Equilibrium time of the pitot-pressure rake was approximately half that of the static-pressure rake (primarily because of the low static pressure).

(c) The pitot tubes could be placed closer together than the static tubes without encountering aerodynamic interference.

pressure gages. Reservoir temperatures were measured with an iron-constantan thermocouple and an automatic temperature recorder.

RESULTS AND DISCUSSION

The calibration of the Ames 10- by 14-inch supersonic wind tunnel consisted of first determining the Mach number and Reynolds number ranges and then making detailed pressure and stream-angle surveys. Except for the determination of the Reynolds number range, tests at each Mach number were conducted at the maximum available Reynolds number. For Mach numbers below 4.4, the nominal reservoir temperature was 60° F. In order to avoid air condensation in the test section at Mach numbers above 4.4, the reservoir temperature was maintained above that corresponding to saturation conditions at the test Mach number (see ref. 1). Steady-state conditions of reservoir pressure and temperature were always established before recording test data.

Mach Number and Reynolds Number Ranges

The Mach number and Reynolds number ranges were determined with the pitot-static-pressure rake (fig. 4) mounted on the tunnel center line of the wind tunnel. Mach numbers were computed from both the ratio of static to reservoir pressure and the ratio of pitot to reservoir pressure.[2] The lowest test Mach number is obtained with the first throat open to its mechanical limit; the highest test Mach number is obtained when the maximum available compression ratio is just sufficient to maintain supersonic flow. The Mach number range of the 10- by 14-inch wind tunnel is 2.7 to 6.3. Nominal test Mach numbers were selected as 2.7, 3.0, 3.5, 4.2, 5.0, and 6.3. The corresponding operating compression ratios for the main diffuser and boundary-layer scoops are given in figure 8. At each Mach number the Reynolds number is varied by varying the reservoir pressure.[3] The ranges of Reynolds number and Mach number are shown in figure 9. The highest Reynolds number of 11.4 million per foot occurs at $M = 3.5$ and the lowest of 1.1 million per foot occurs at $M = 5.0$.

---

[2]As pointed out in reference 1, Mach numbers computed by the two methods agree for flow free of air condensation. Such was the case here; the agreement was within ±0.02 Mach number in all cases.

[3]Reynolds number variation can also be obtained by varying the reservoir temperatures; however, the capacity of the present supply air heater is such that only at $M = 4.2$ and 5.0 could appreciable changes in Reynolds number be realized. The data presented are for a constant reservoir temperature at each nominal Mach number.

Pressure Survey

Static-pressure distributions.- The results of the survey with the pitot-pressure rake (fig. 5) converted to stream static-pressure coefficient are presented in figures 10 through 12. The reference point for the pressure coefficient is located at the intersection of the tunnel center line and the center line of the windows ($x = 0$). As was discussed previously, the static-pressure rake was used only to check the pitot-pressure measurements and thereby to ascertain if the flow was free of condensed air. Comparison of the results obtained with the two rakes revealed no air condensation, the pressure coefficients (calculated with the aid of the Rayleigh formula in the case of pitot pressure) agreeing within experimental scatter.

Typical results of the pressure survey for one Mach number and in one plane normal to the wind-tunnel center line are presented in figure 10. These results show that, although the flow is not two-dimensional (see fig. 10, $\theta = 0^\circ$), it is symmetrical about the horizontal and vertical planes containing the tunnel center line. For this reason, the remaining data are presented for one quadrant only - the upper right quadrant when viewed from a downstream position (see fig. 3).

Longitudinal distributions of stream static-pressure coefficient are presented in figure 11. Results are shown for the tunnel center line and lines 1 and 2 inches off the center line in both the horizontal and vertical planes (i.e., $r = 0$, $\theta = 0^\circ$; $r = 1$, $\theta = 0^\circ$; $r = 2$, $\theta = 0^\circ$; $r = 1$, $\theta = 90^\circ$; $r = 2$, $\theta = 90^\circ$). The results shown in figure 11 indicate that, in general, the flow in the test section is reasonably uniform over a length approximately equal to one test-section width. There are exceptions, however. For example, at the lowest Mach number, $M = 2.7$, a relatively strong pressure gradient appears off the center line in the vertical plane (see curve for $r = 2$, $\theta = 90^\circ$). Though there is no direct evidence, the major cause of this gradient is believed to be flow separation just downstream of the sonic throat. The general decrease in static pressure in the region from $x = -9$ to $x = 3$ at $M = 2.7$ and 3.0 results from "expanding" flow in the test section. It was not possible to eliminate this situation, inasmuch as decreasing the second-throat area caused the tunnel to choke.

Radial variations of stream static-pressure coefficient are presented in figure 12. Distributions are shown at three longitudinal stations and for four rake angular positions. Another exception to the general uniformity of the flow can be noted at $M = 6.3$ (see fig. 12(f)). The gradients in this case appear primarily in the horizontal plane (see $\theta = 0^\circ$ and 30°). The rapid build-up of the side-wall boundary layer caused by transverse pressure gradients in the effuser (see ref. 4) is believed to be the cause of these pressure gradients.

The static-pressure distributions reveal that, over most of the region about one test-section width in length and extending ±2 inches vertically and ±2 inches horizontally from the tunnel center line, the flow in the 10- by 14-inch wind tunnel has sufficient uniformity for test purposes over the Mach number range of 2.7 to 6.3. For example, the pressure distributions just presented were employed to determine the buoyancy correction to the zero-lift foredrag of a typical test body, namely, a fineness-ratio-10, 1-inch-diameter cone cylinder, having a conical nose of fineness ratio 3 and located in the wind tunnel between $x = -8$ and $x = 2$. This investigation revealed that the maximum correction was approximately 3 percent of the measured foredrag (not including base drag) at zero lift over the entire test Mach number range.[4] Models tested at angle of attack are pitched in the horizontal ($\theta = 0^\circ$) plane with the center of rotation of the angle-of-attack mechanism at $x = 0$. With this arrangement, appreciable pressure gradients are not encountered until the model reaches an angle of attack of about 20°. At this angle of attack, the aerodynamic forces are generally so large that the buoyancy corrections are again only a small percentage.

Mach number distributions.- The results of the pressure survey are also presented in the form of Mach number distributions along the tunnel center line of the wind tunnel in figure 13. Examination of figure 13 reveals that the variation in Mach number along the center line is less than ±1 percent at the lower Mach numbers, less than ±0.5 percent at the intermediate Mach numbers, and reaches a maximum of only ±2 percent at the highest test Mach number.

Stream-Angle Survey

Results of the stream-angle survey are presented in figure 14.[5] Longitudinal distributions are shown for the tunnel center line and lines 1 and 2 inches off the center line in both the horizontal and vertical planes (i.e., the same lines as the static-pressure coefficient, $r = 0$, $\theta = 0^\circ$; $r = 1$, $\theta = 0^\circ$; $r = 2$, $\theta = 0^\circ$; $r = 1$, $\theta = 90^\circ$; $r = 2$, $\theta = 90^\circ$). The variation in stream angle along the tunnel center line ($r = 0$, $\theta = 0^\circ$) of the wind tunnel is generally within the measuring accuracy of the stream-angle rake, being less than $\pm 0.2^\circ$ at all Mach numbers. Off the center line, stream-angle gradients appear in the vertical plane at the lower Mach numbers and in the horizontal plane at the higher Mach numbers. These gradients can be related to the previously observed pressure gradients. With models pitched in the horizontal plane, the stream-angle variations at low Mach numbers are too far off the center line to

[4]The reference point for the drag correction was taken as the apex of the cone.

[5]Following the procedure established in the pressure survey, distributions are shown only for the upper right quadrant of the test section (viewed from a downstream position).

affect the flow about a test body and would be in the spanwise direction for wings. The variations in the horizontal plane at high Mach numbers could have an appreciable effect; again, however, a model would not encounter these stream irregularities until pitched to a relatively large angle of attack, and, in this case, the large aerodynamic forces would minimize the effects on a percentage basis.

CONCLUDING REMARKS

The Ames 10- by 14-inch supersonic wind tunnel is described in some detail. Pertinent features of the design and operation of this facility are included. The wind tunnel has a Mach number range of 2.7 to 6.3 with a Reynolds number range of 1 million to 11 million per foot, depending on Mach number and reservoir pressure. Nominal test Mach numbers are 2.7, 3.0, 3.5, 4.2, 5.0, and 6.3.

Pressure surveys revealed that, with but few exceptions, the flow in the test section is sufficiently uniform for test purposes within a region about one test-section width in length and extending ±2 inches vertically and ±2 inches horizontally from the tunnel center line. By way of example, the buoyancy correction to the zero-lift foredrag of a 10-inch long, 1-inch-diameter body of revolution is 3 percent or less at all test Mach numbers. The Mach number variation along the tunnel center line of the test section is less than ±1 percent at low Mach numbers, less than ±0.5 percent at intermediate Mach numbers, and reaches a maximum of ±2 percent at the highest test Mach number.

The variation in stream angle along the tunnel center line is less than $\pm 0.2^{\circ}$ at all Mach numbers. Since models are pitched in the horizontal plane, stream-angle (and pressure) gradients observed off the center line in the vertical plane at the lower test Mach numbers do not appreciably affect the flow about a test body and are in the spanwise direction for wings. Similar gradients observed in the horizontal plane at the higher test Mach numbers are generally of little consequence since they are not encountered by a model until it is pitched to an angle of attack of about 20°.

In addition to the fact that the "scissors-type" nozzle used in the 10- by 14-inch wind tunnel is a simple mechanism, it has two advantages:

1. Supersonic flow may be established at a relatively low Mach number by simply opening the nozzle blocks. In this manner, the large starting compression ratios associated with establishing supersonic flow at high Mach numbers are avoided.

2. After supersonic flow has been established, the test-section Mach number is readily increased by simply closing the nozzle blocks. At the same time the second-throat area is maintained at a value for efficient diffusion.

Ames Aeronautical Laboratory
National Advisory Committee for Aeronautics
Moffett Field, Calif., Nov. 3, 1953

APPENDIX

SYMBOLS

H	total pressure, lb/sq in.
H'	total pressure behind a normal shock, lb/sq in.
M	Mach number
p	static pressure, lb/sq in.
P	stream static-pressure coefficient, $\frac{p - p_R}{q_R}$
q	dynamic pressure, lb/sq in.
x,r,θ	cylindrical coordinates of a point in the test section, in. and deg, respectively (see fig. 3)
y	distance normal to horizontal plane of symmetry of nozzle, in.
T	total temperature, ^{o}F
ϵ	stream angle, positive for upflow or flow toward the right when viewed from a downstream position, deg

Subscripts

d	quantity measured in the main diffuser exhaust line
o	quantity measured in the reservoir
R	quantity evaluated at origin of nozzle coordinate system (see fig. 3)
s	quantity measured in the boundary-layer-scoop exhaust line

REFERENCES

1. Hansen, C. Frederick, and Nothwang, George J.: Condensation of Air in Supersonic Wind Tunnels and Its Effects on Flow About Models. NACA TN 2690, 1952.

2. Dimeff, John, Hallett, Ralph K., Jr., and Hansen, C. Frederick: X-Ray Instrumentation for Density Measurements in a Supersonic Flow Field. NACA TN 2845, 1952.

3. McLellan, Charles H., Williams, Thomas W., and Beckwith, Ivan E.: Investigation of the Flow Through a Single-Stage Two-Dimensional Nozzle in the Langley 11-Inch Hypersonic Tunnel. NACA TN 2223, 1950.

4. Haefeli, Rudolph C.: Use of Fences to Increase Uniformity of Boundary Layer on Sidewalls of Supersonic Wind Tunnels. NACA RM E52E19, 1952.

TABLE I.- COORDINATES OF NOZZLE BLOCKS

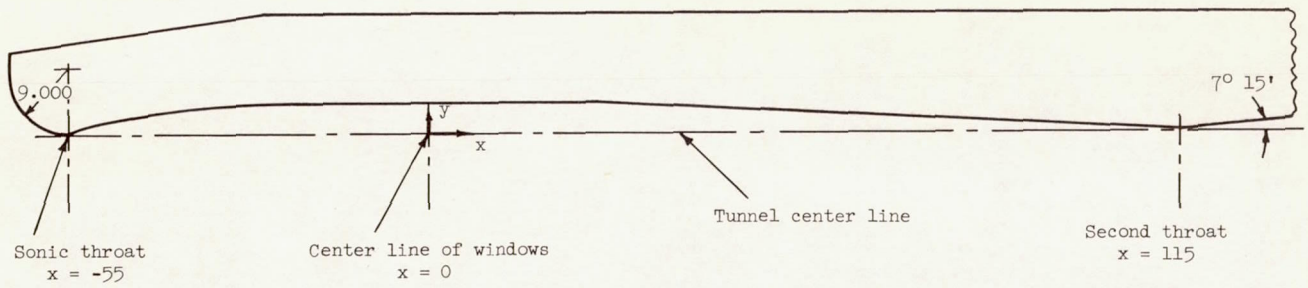

x	y	x	y	x	y	x	y	x	y	x	y	x	y	x	y
-55.000	0.218	-54.420	0.357	-53.600	0.675	-51.300	1.391	-48.400	2.081	-43.250	2.927	-32.000	3.964	-17.500	4.514
-54.980	.218	-54.400	.366	-53.550	.692	-51.200	1.419	-48.300	2.102	-43.000	2.959	-31.500	3.995	-17.000	4.522
-54.960	.218	-54.380	.375	-53.500	.710	-51.100	1.446	-48.200	2.122	-42.750	2.991	-31.000	4.025	-16.500	4.528
-54.940	.219	-54.360	.383	-53.450	.728	-51.000	1.472	-48.100	2.142	-42.500	3.022	-30.500	4.054	-16.000	4.534
-54.920	.219	-54.340	.392	-53.400	.745	-50.900	1.499	-48.000	2.162	-42.250	3.052	-30.000	4.083	-15.500	4.540
-54.900	.220	-54.320	.400	-53.350	.762	-50.800	1.525	-47.900	2.182	-42.000	3.083	-29.500	4.110	-15.000	4.545
-54.880	.222	-54.300	.408	-53.300	.780	-50.700	1.551	-47.800	2.201	-41.750	3.112	-29.000	4.136	Straight line	
-54.860	.223	-54.280	.417	-53.250	.797	-50.600	1.557	-47.700	2.221	-41.500	3.141	-28.500	4.162	9.000	4.764
-54.840	.226	-54.260	.425	-53.200	.814	-50.500	1.602	-47.600	2.240	-41.250	3.170	-28.000	4.186	10.000	4.770
-54.820	.229	-54.240	.433	-53.150	.831	-50.400	1.627	-47.500	2.259	-41.000	3.198	-27.500	4.210	11.000	4.772
-54.800	.232	-54.220	.441	-53.100	.847	-50.300	1.652	-47.400	2.278	-40.750	3.226	-27.000	4.233	12.000	4.769
-54.780	.236	-54.200	.449	-53.050	.864	-50.200	1.677	-47.300	2.296	-40.500	3.253	-26.500	4.255	13.000	4.762
-54.760	.240	-54.180	.457	-53.000	.881	-50.100	1.701	-47.200	2.315	-40.250	3.280	-26.000	4.276	14.000	4.749
-54.740	.245	-54.160	.465	-52.900	.913	-50.000	1.725	-47.100	2.333	-40.000	3.306	-25.500	4.296	15.000	4.732
-54.720	.250	-54.140	.473	-52.800	.946	-49.900	1.749	-47.000	2.351	-39.500	3.358	-25.000	4.316	16.000	4.710
-54.700	.255	-54.120	.481	-52.700	.978	-49.800	1.773	-46.750	2.396	-39.000	3.408	-24.500	4.334	17.000	4.684
-54.680	.261	-54.100	.489	-52.600	1.010	-49.700	1.797	-46.500	2.440	-38.500	3.457	-24.000	4.352	18.000	4.652
-54.660	.266	-54.080	.497	-52.500	1.041	-49.600	1.820	-46.250	2.483	-38.000	3.504	-23.500	4.369	19.000	4.616
-54.640	.273	-54.060	.504	-52.400	1.072	-49.500	1.843	-46.000	2.524	-37.500	3.550	-23.000	4.385	20.000	4.575
-54.620	.279	-54.040	.512	-52.300	1.103	-49.400	1.866	-45.750	2.565	-37.000	3.594	-22.500	4.401	20.993	4.529
-54.600	.286	-54.020	.520	-52.200	1.133	-49.300	1.888	-45.500	2.605	-36.500	3.636	-22.000	4.415	Straight line	
-54.580	.293	-54.000	.527	-52.100	1.163	-49.200	1.910	-45.250	2.644	-36.000	3.677	-21.500	4.429	106.703	.400
-54.560	.300	-53.950	.546	-52.000	1.193	-49.100	1.933	-45.000	2.682	-35.500	3.717	-21.000	4.442	108.000	.342
-54.540	.308	-53.900	.565	-51.900	1.222	-49.000	1.954	-44.750	2.720	-35.000	3.756	-20.500	4.455	109.000	.304
-54.520	.316	-53.850	.584	-51.800	1.251	-48.900	1.976	-44.500	2.756	-34.500	3.793	-20.000	4.466	110.000	.273
-54.500	.324	-53.800	.602	-51.700	1.280	-48.800	1.998	-44.250	2.791	-34.000	3.829	-19.500	4.477	111.000	.246
-54.480	.332	-53.750	.621	-51.600	1.308	-48.700	2.019	-44.000	2.826	-33.500	3.864	-19.000	4.488	112.000	.226
-54.460	.340	-53.700	.639	-51.500	1.336	-48.600	2.040	-43.750	2.860	-33.000	3.898	-18.500	4.497	113.000	.212
-54.440	.349	-53.650	.657	-51.400	1.364	-48.500	2.061	-43.500	2.894	-32.500	3.932	-18.000	4.506	114.000	.203
														115.000	.200

NACA

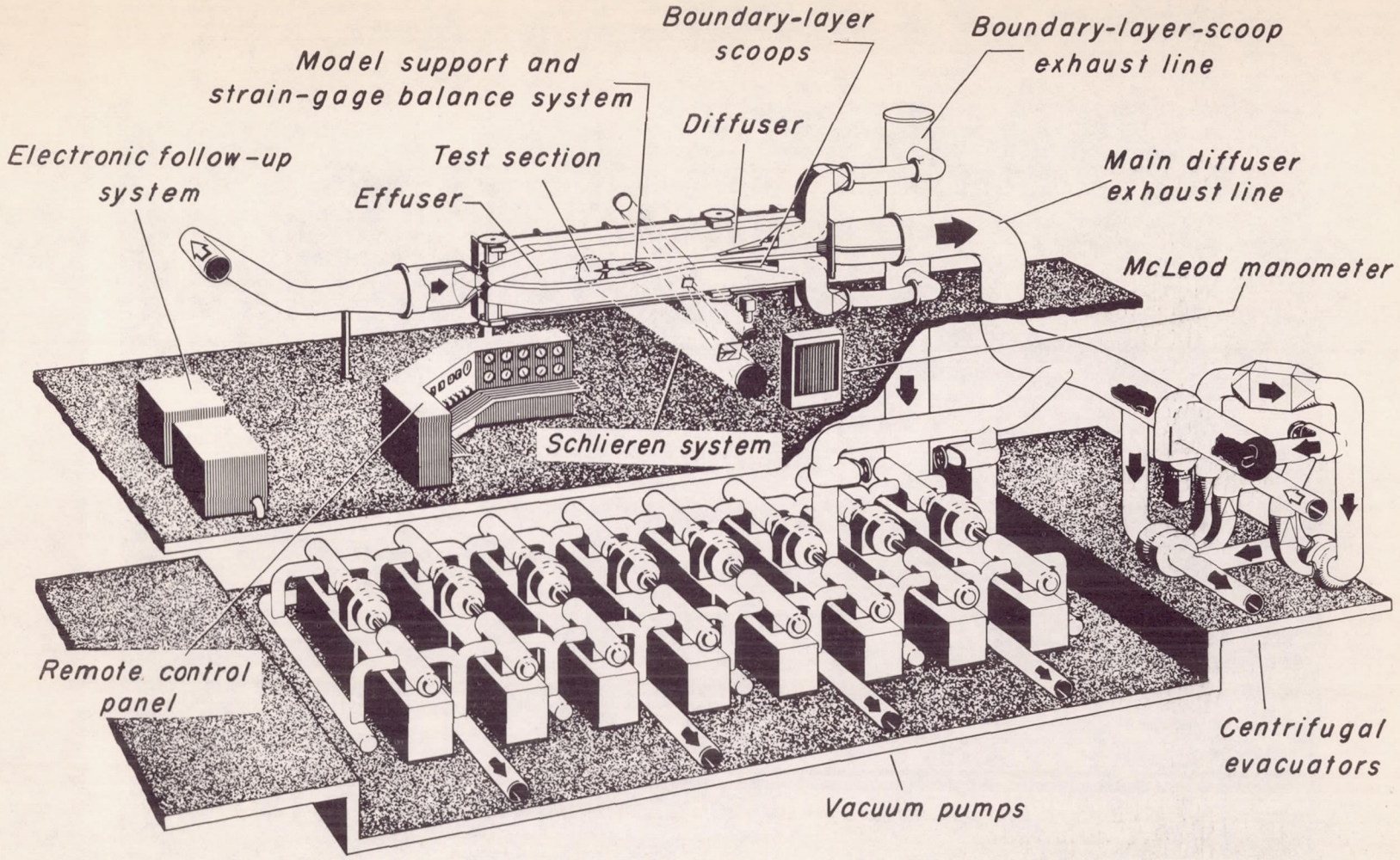

Figure 1.- Schematic view of the 10- by 14-inch supersonic wind tunnel.

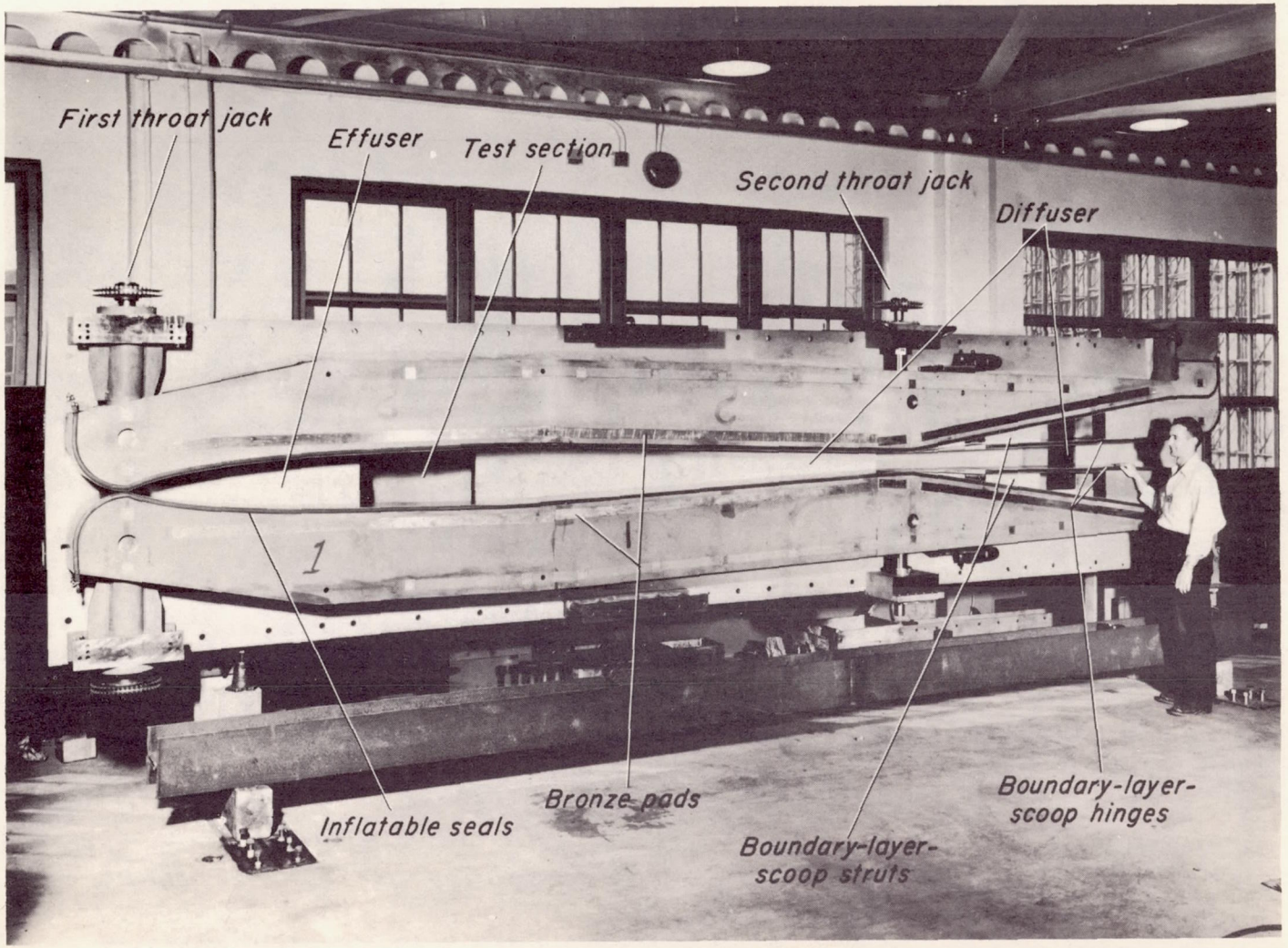

Figure 2.- The nozzle of the Ames 10- by 14-inch supersonic wind tunnel with one side wall removed.

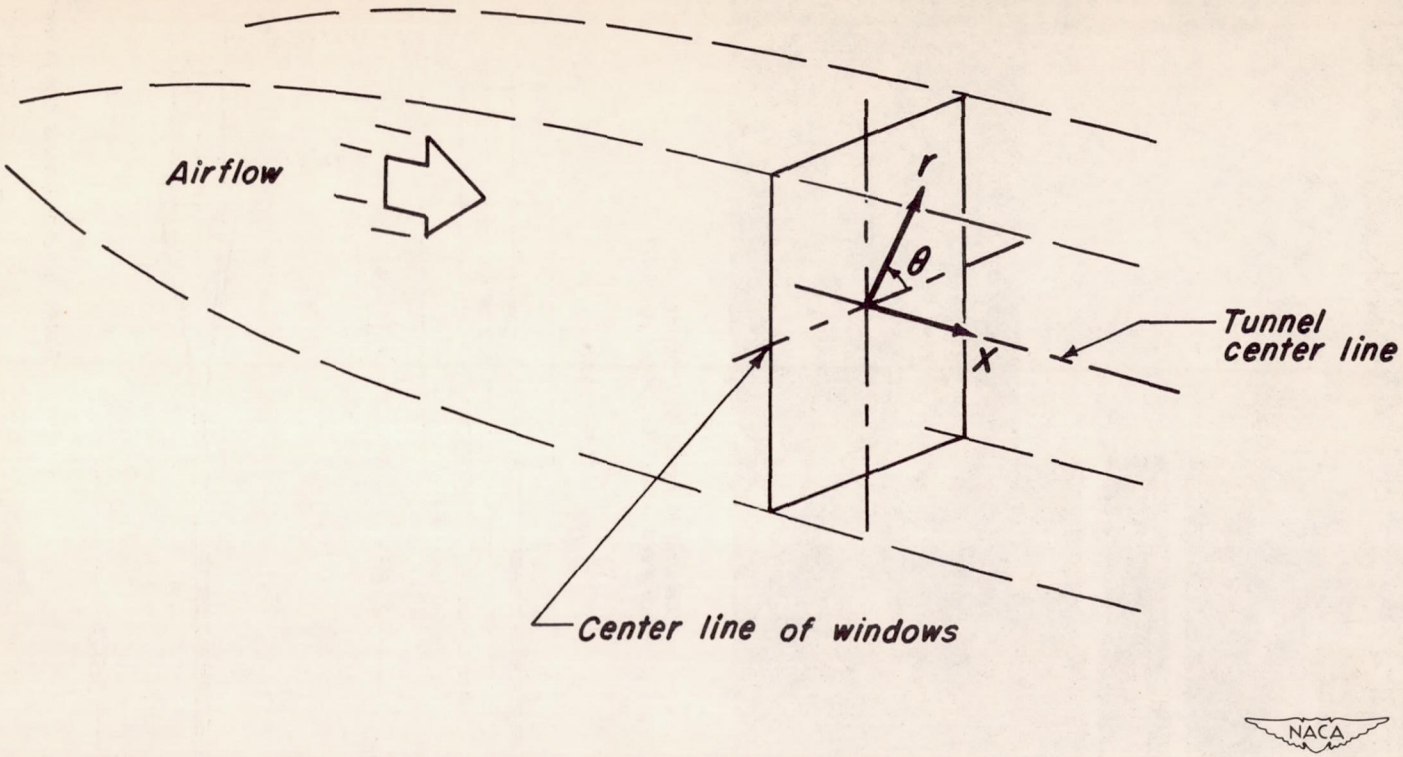

Figure 3.– Coordinate system for points in the test section.

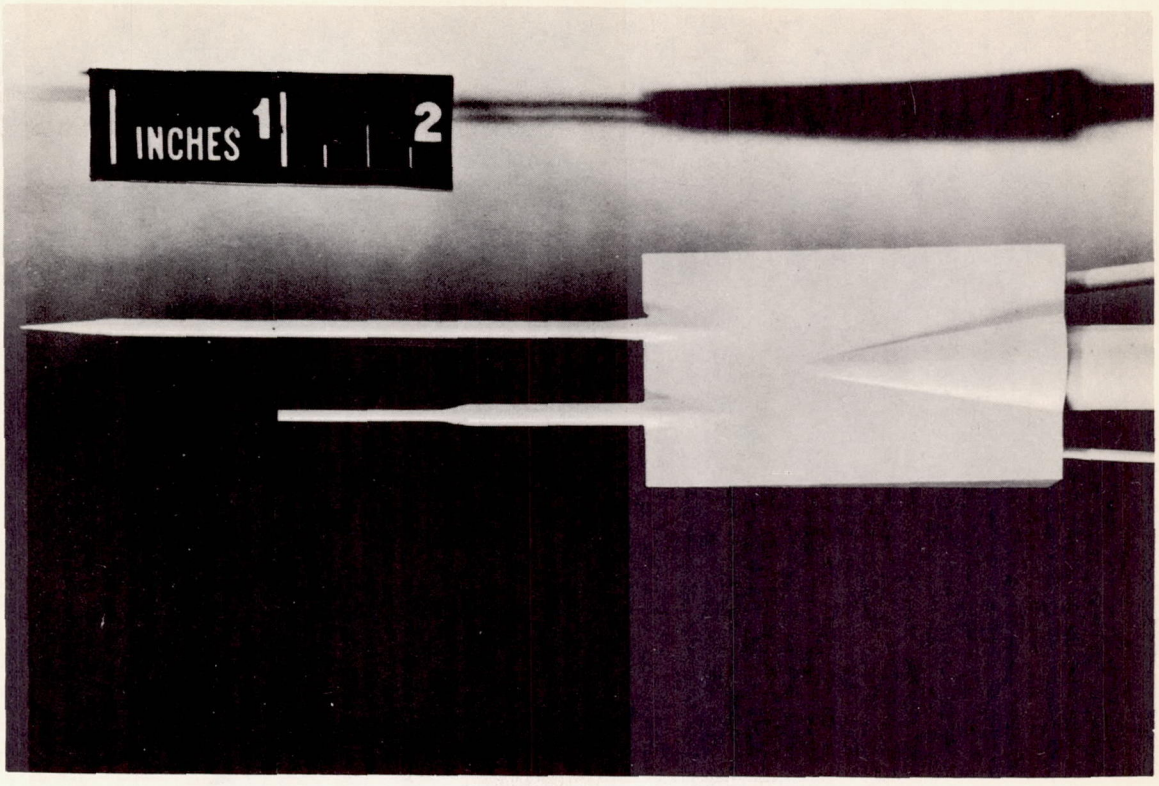

A-18496.1

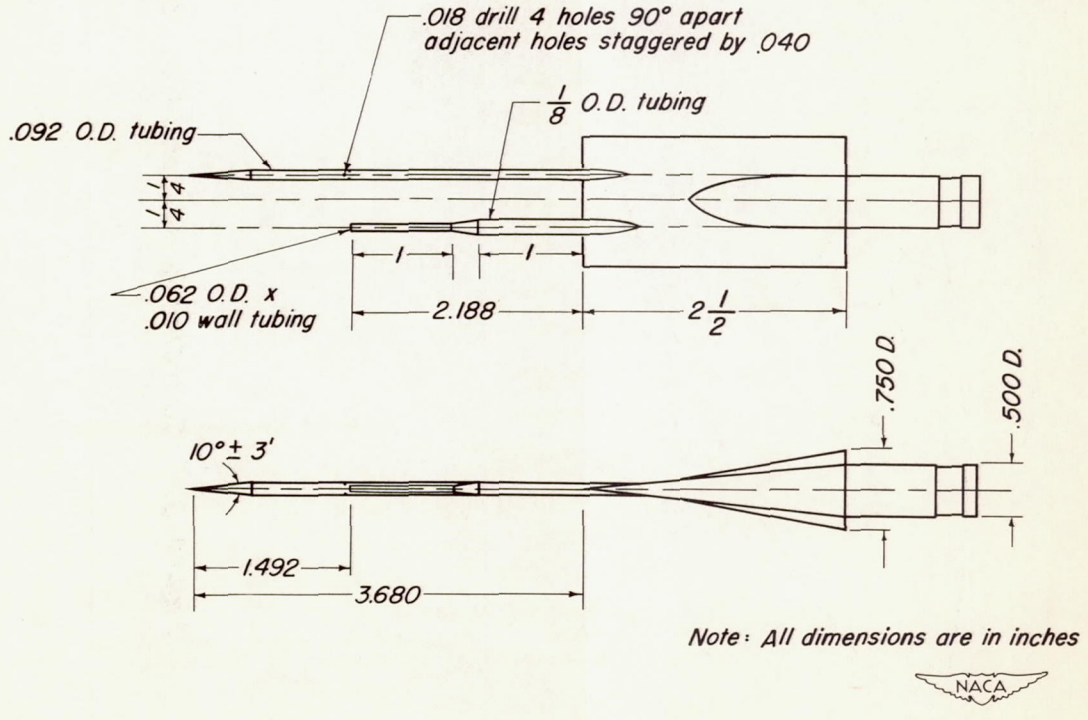

Figure 4.— Pitot-static-pressure rake.

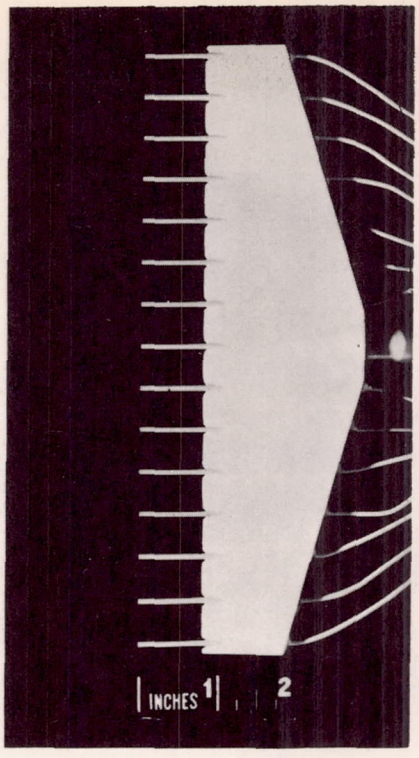

A-18504.1

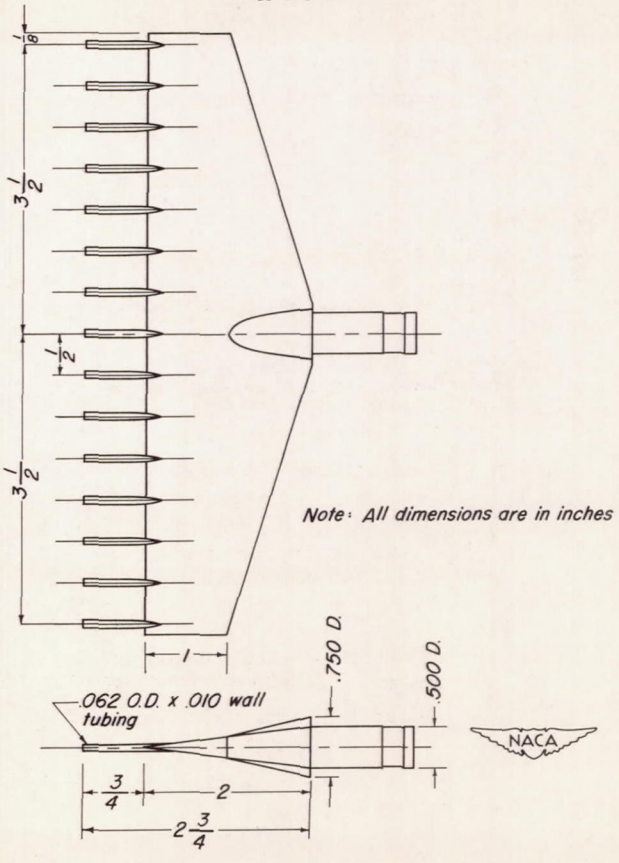

Figure 5.- Pitot-pressure survey rake.

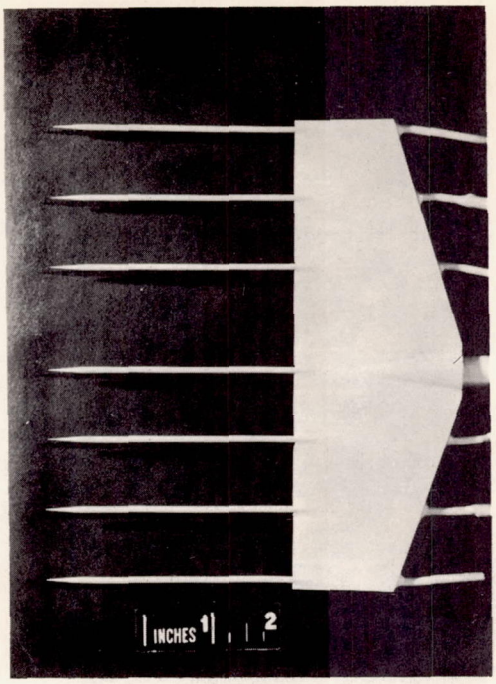

A-18505.1

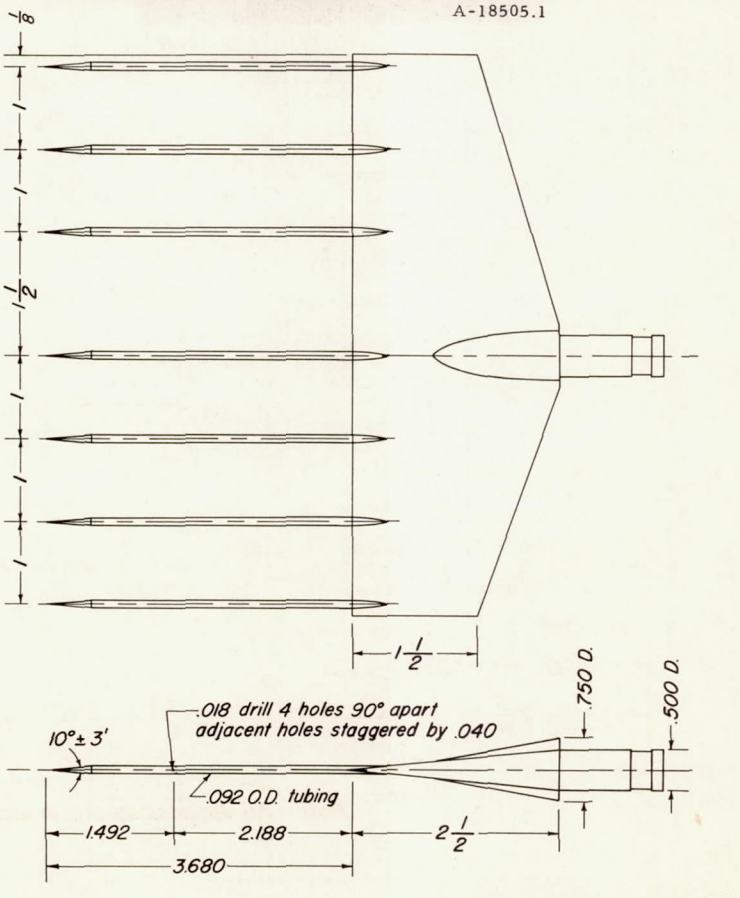

Note: All dimensions are in inches

NACA

Figure 6.- Static-pressure survey rake.

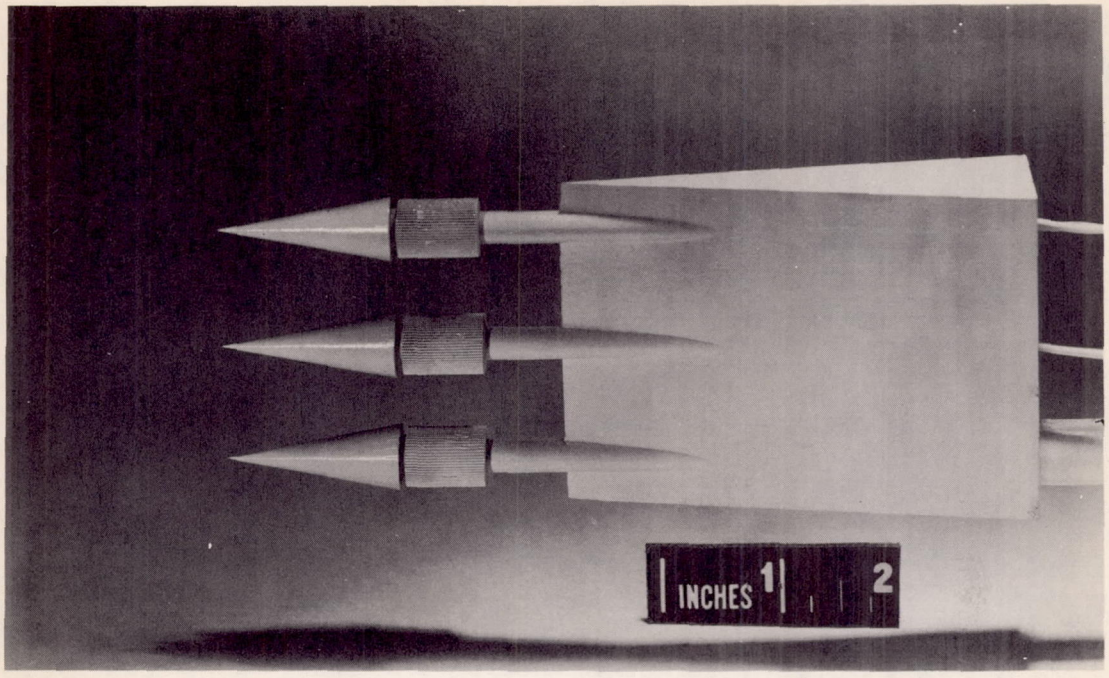

A-18497

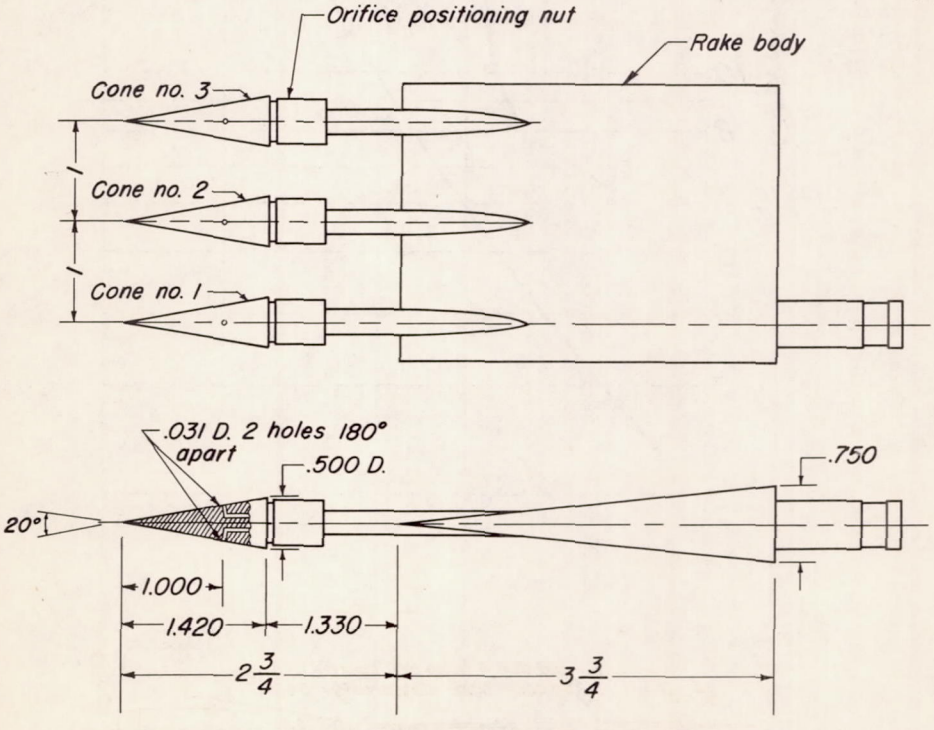

Figure 7.– Stream-angle survey rake.

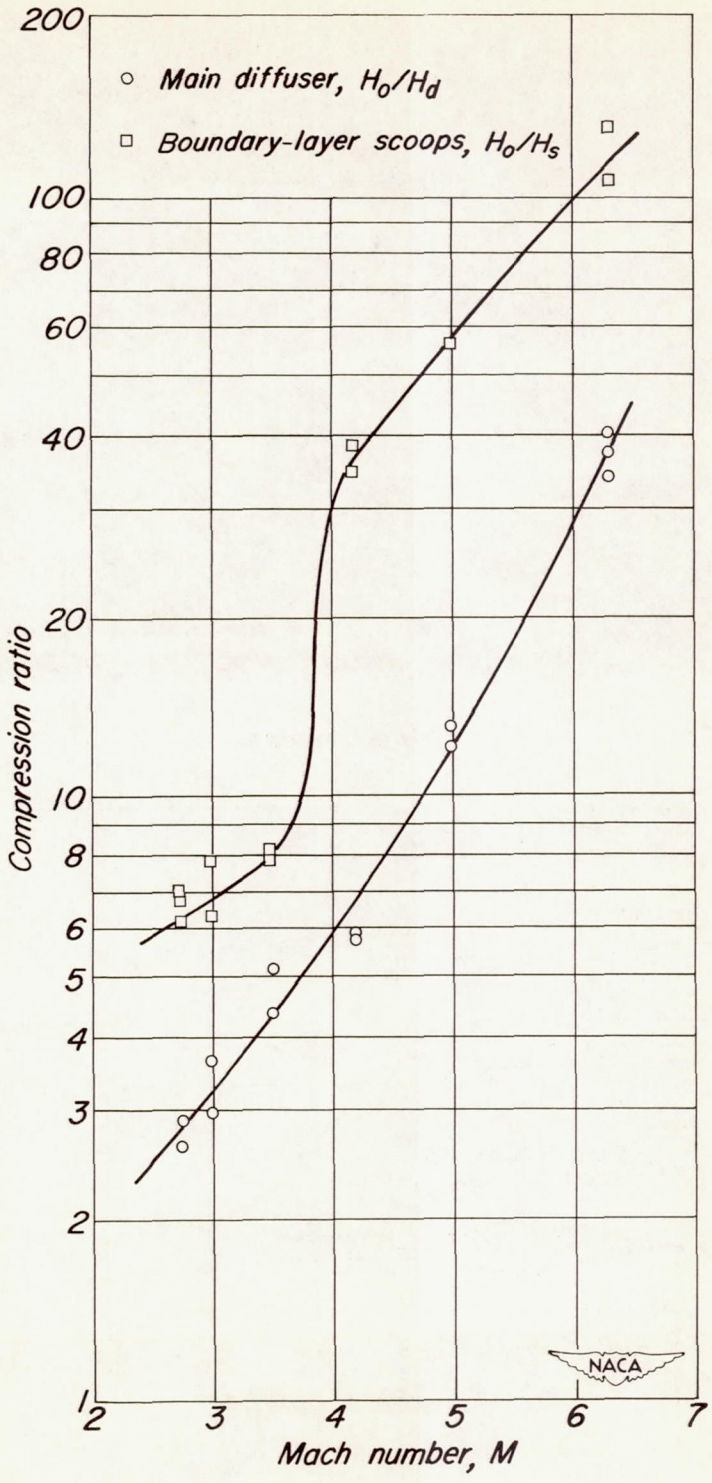

Figure 8.- Compression ratios used in normal operation of the Ames 10- by 14- inch supersonic wind tunnel.

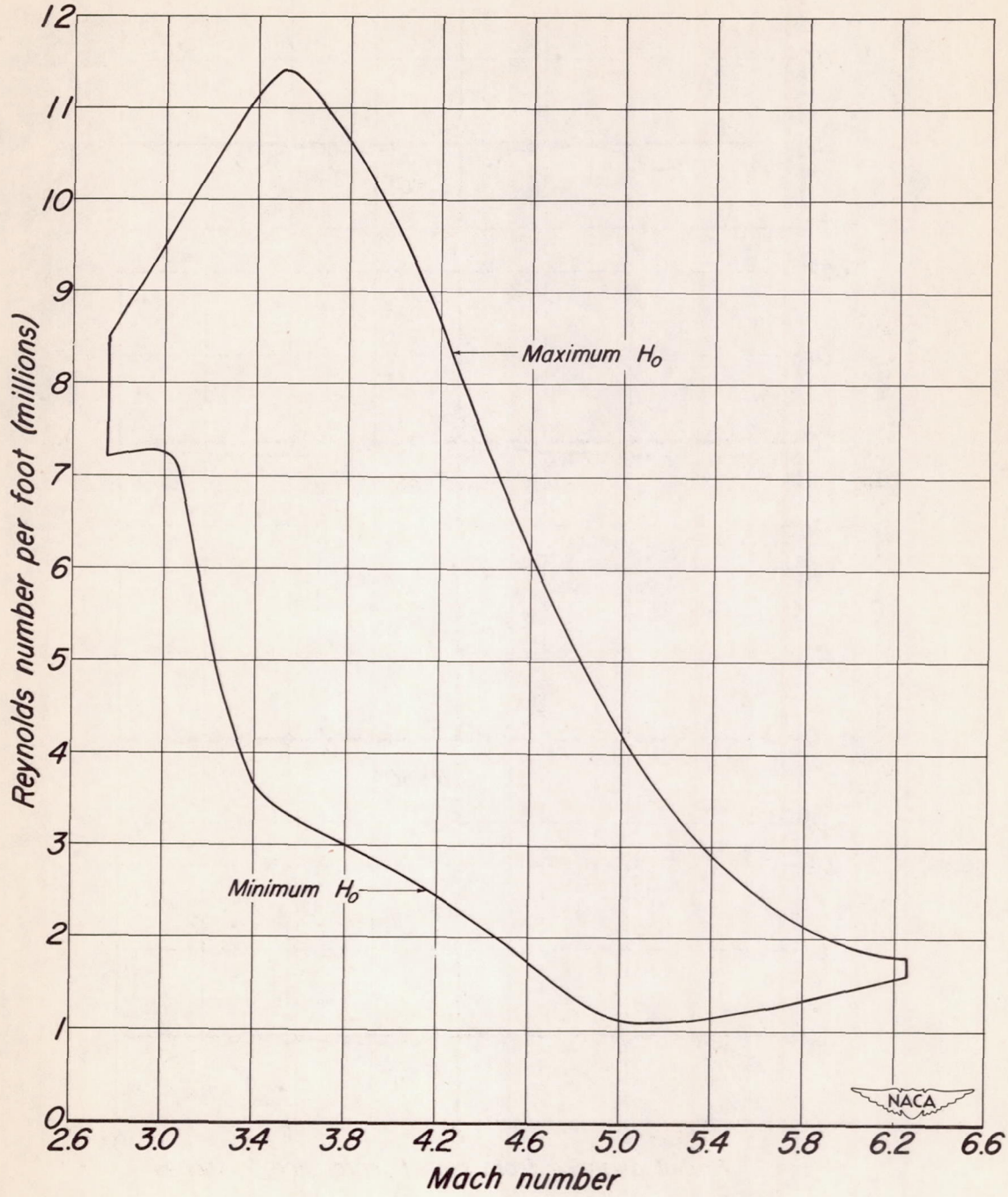

Figure 9.– Reynolds number and Mach number ranges of the Ames 10– by 14– inch supersonic wind tunnel.

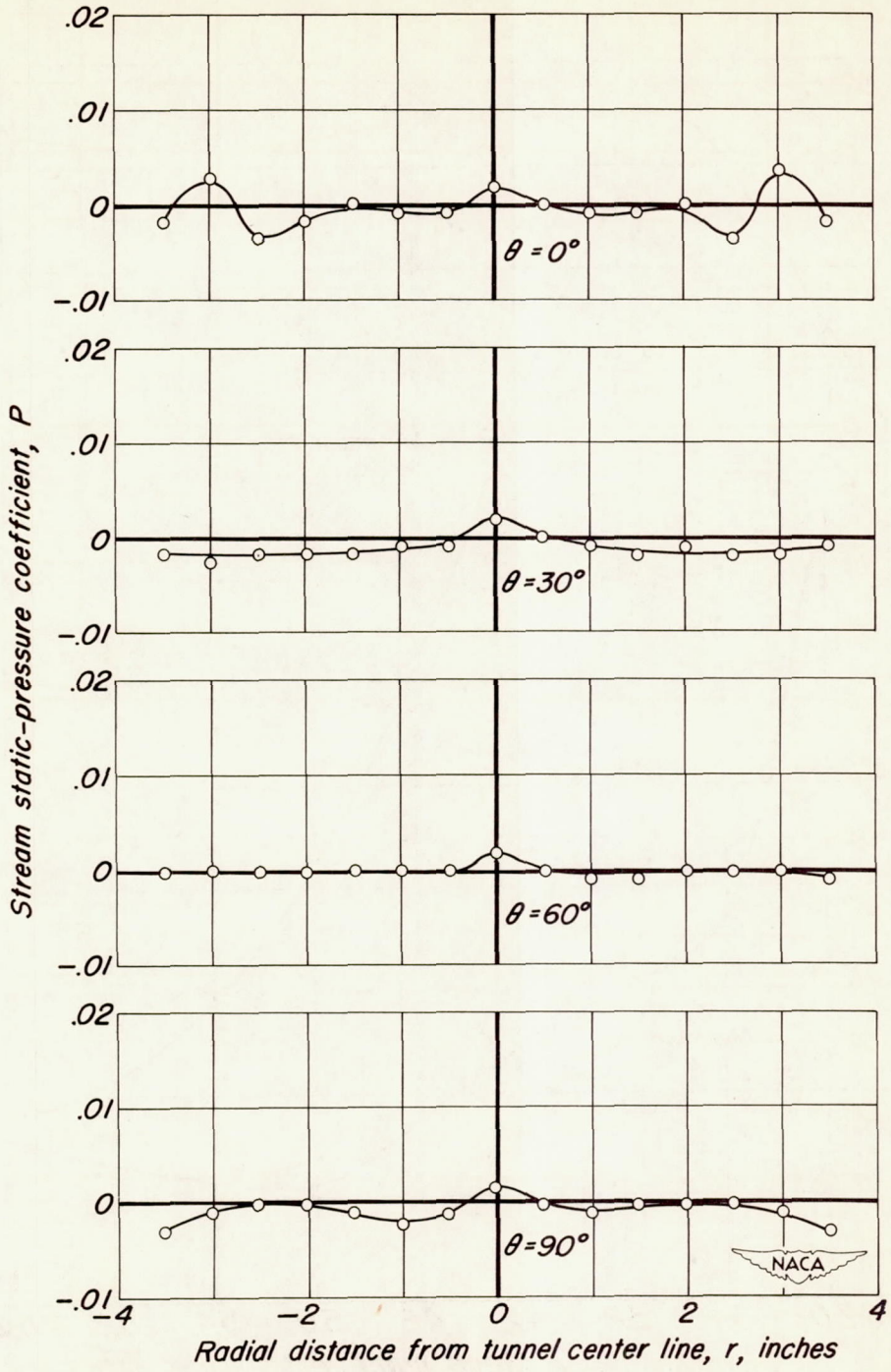

Figure 10.– Radial variation of stream static-pressure coefficient in the Ames 10- by 14- inch supersonic wind tunnel; M = 3.5, H_0 = 82 lb/sq in. abs., T_0 = 60° F, x = −3.

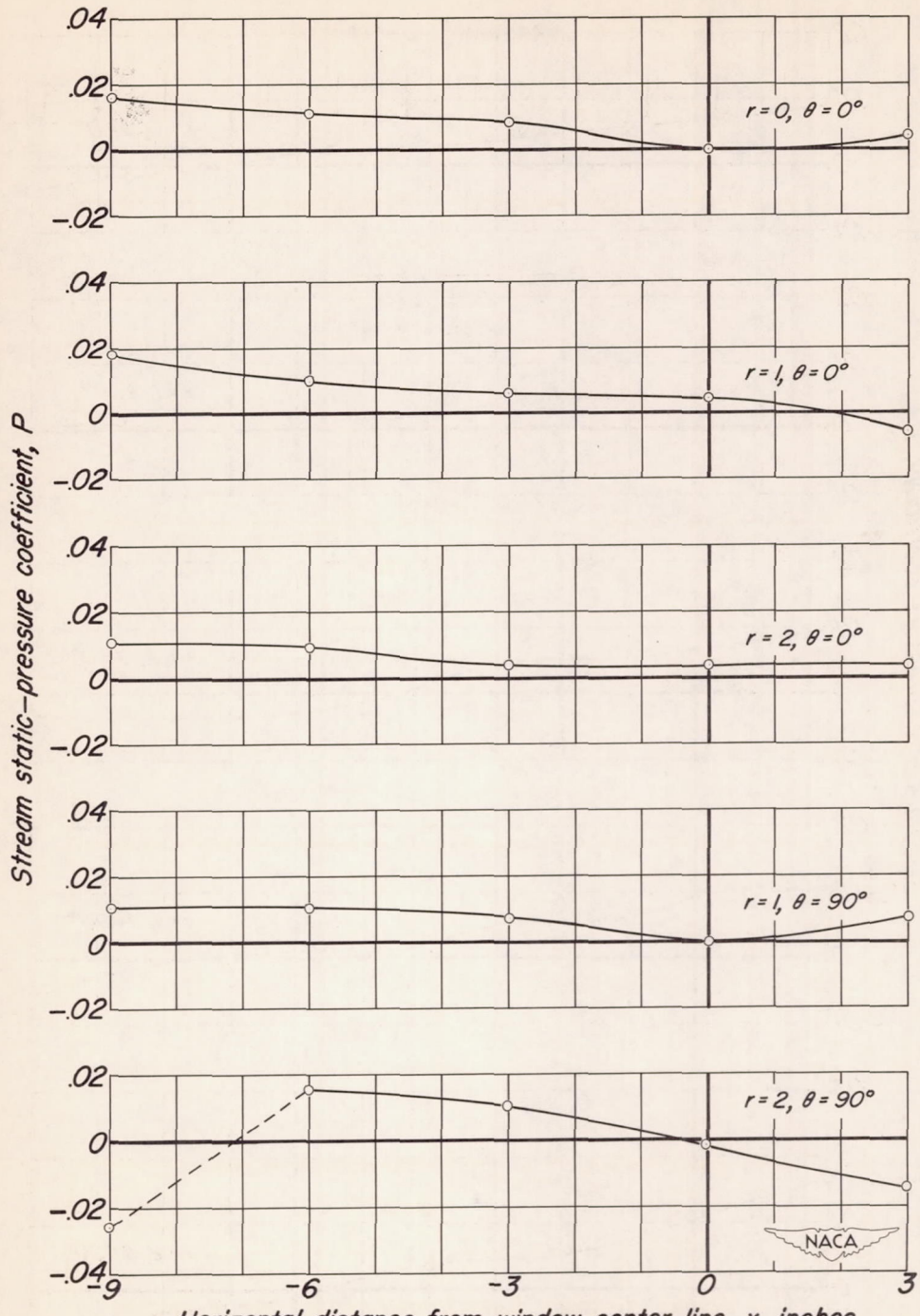

(a) $M = 2.7$, $H_0 = 42$ lb/sq in. abs., $T_0 = 60°$ F

Figure 11.– Longitudinal variation of stream static-pressure coefficient in the Ames 10- by 14- inch supersonic wind tunnel.

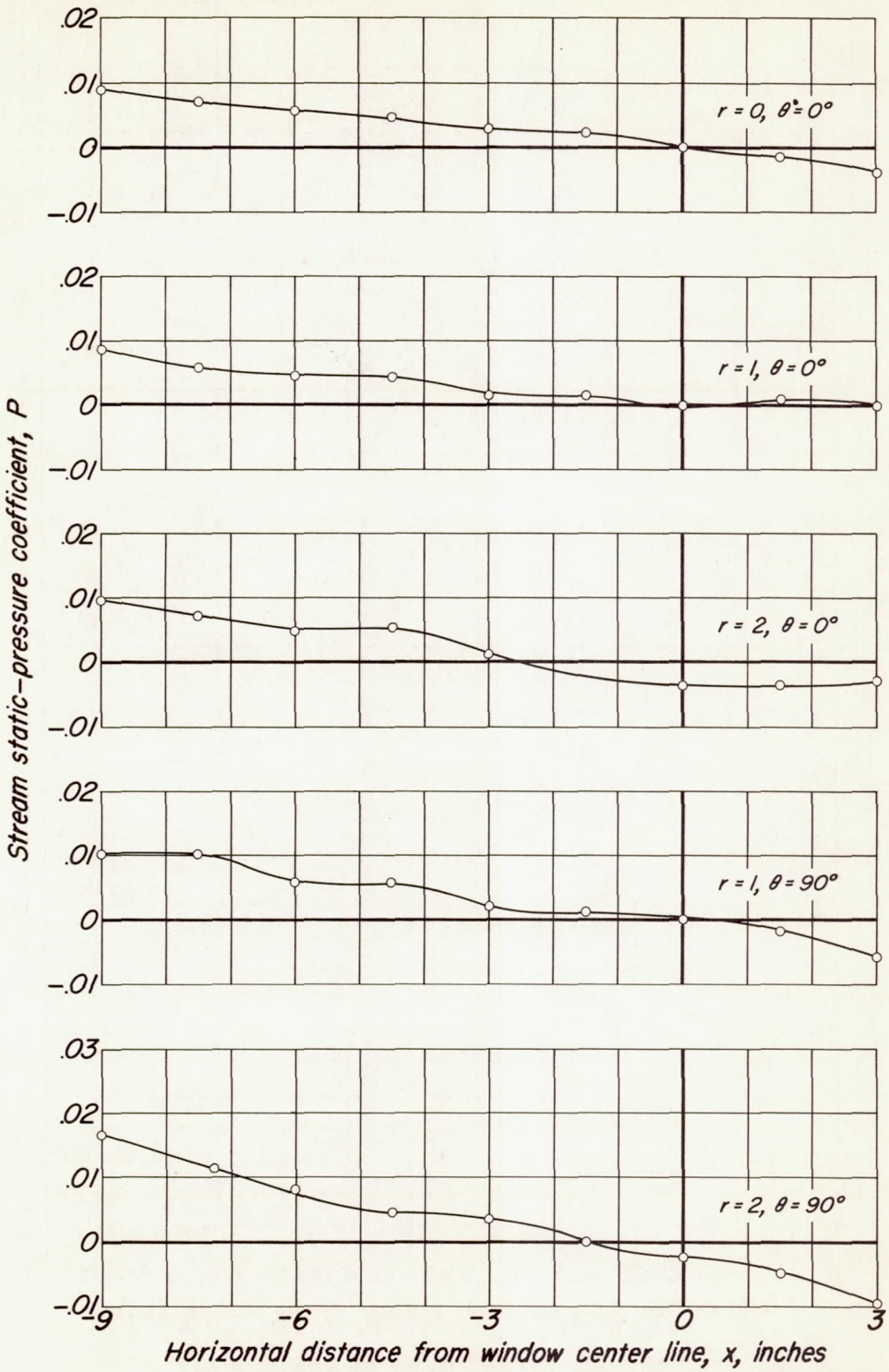

(b) $M = 3.0$, $H_o = 55$ lb/sq in. abs., $T_o = 60°$ F

Figure 11.– Continued.

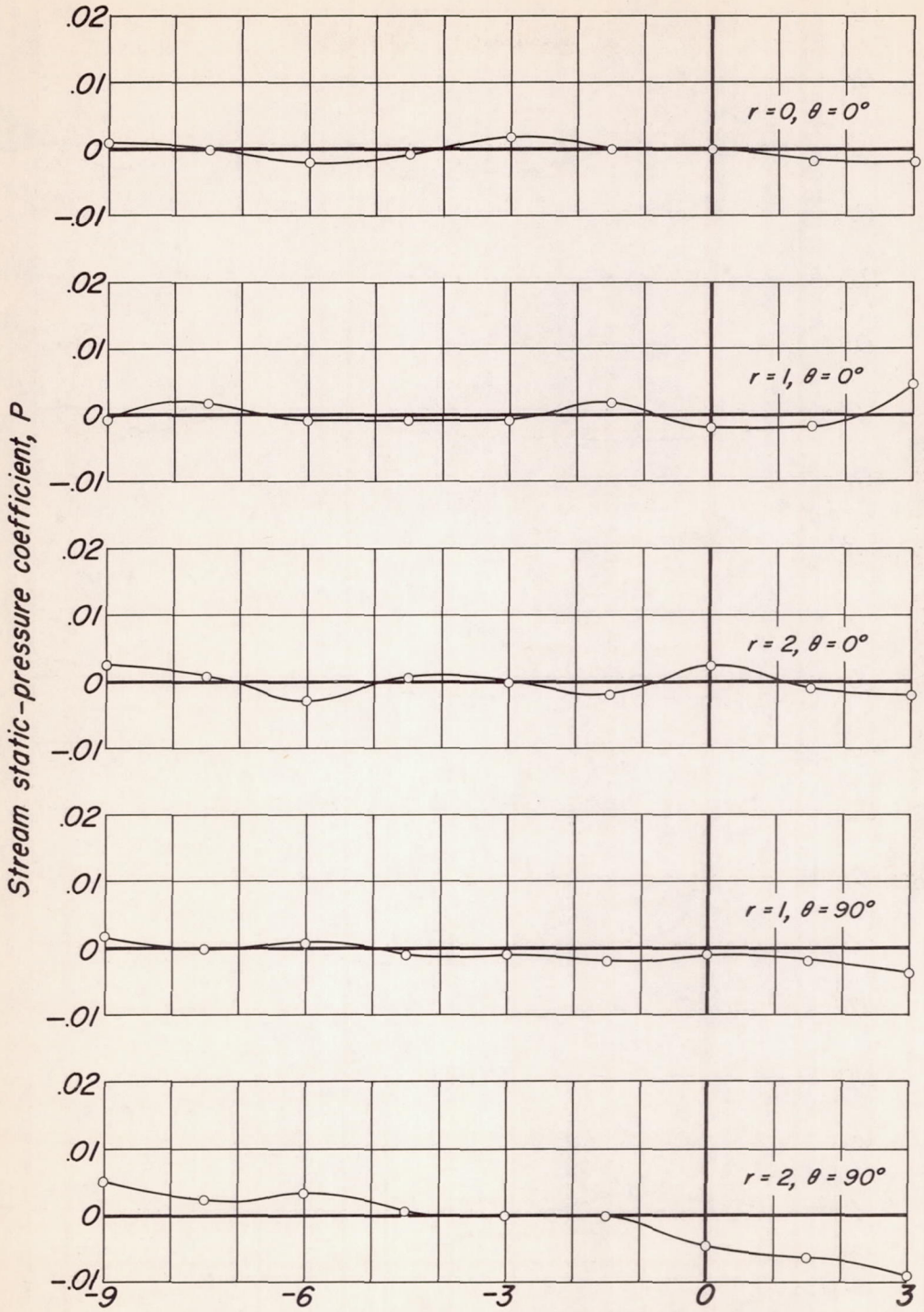

(c) $M = 3.5$, $H_0 = 82$ lb/sq in. abs., $T_0 = 60°$ F

NACA

Figure 11.- Continued.

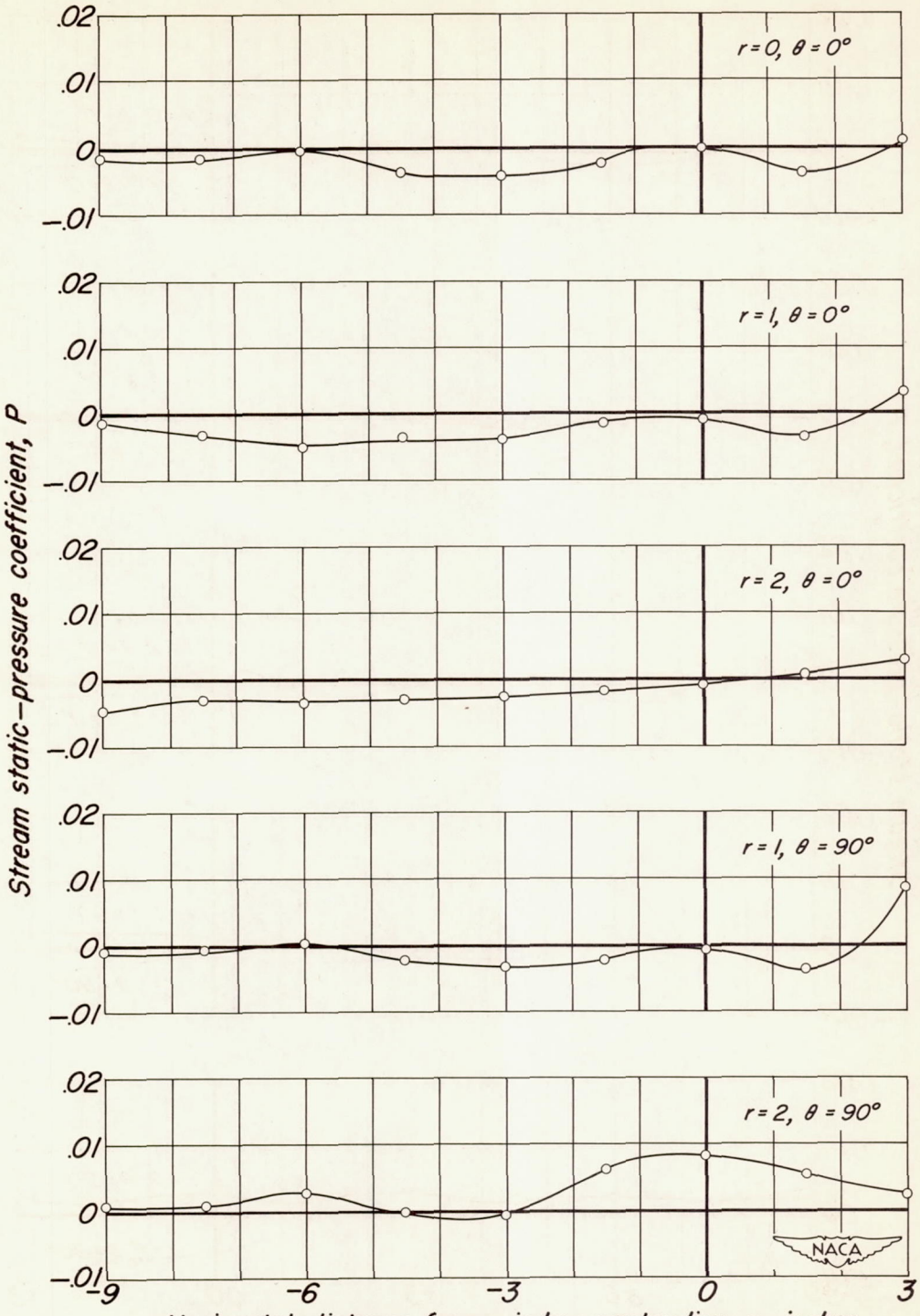

(d) $M = 4.2$, $H_o = 88$ lb/sq in. abs., $T_o = 60°$ F

Figure 11.- Continued.

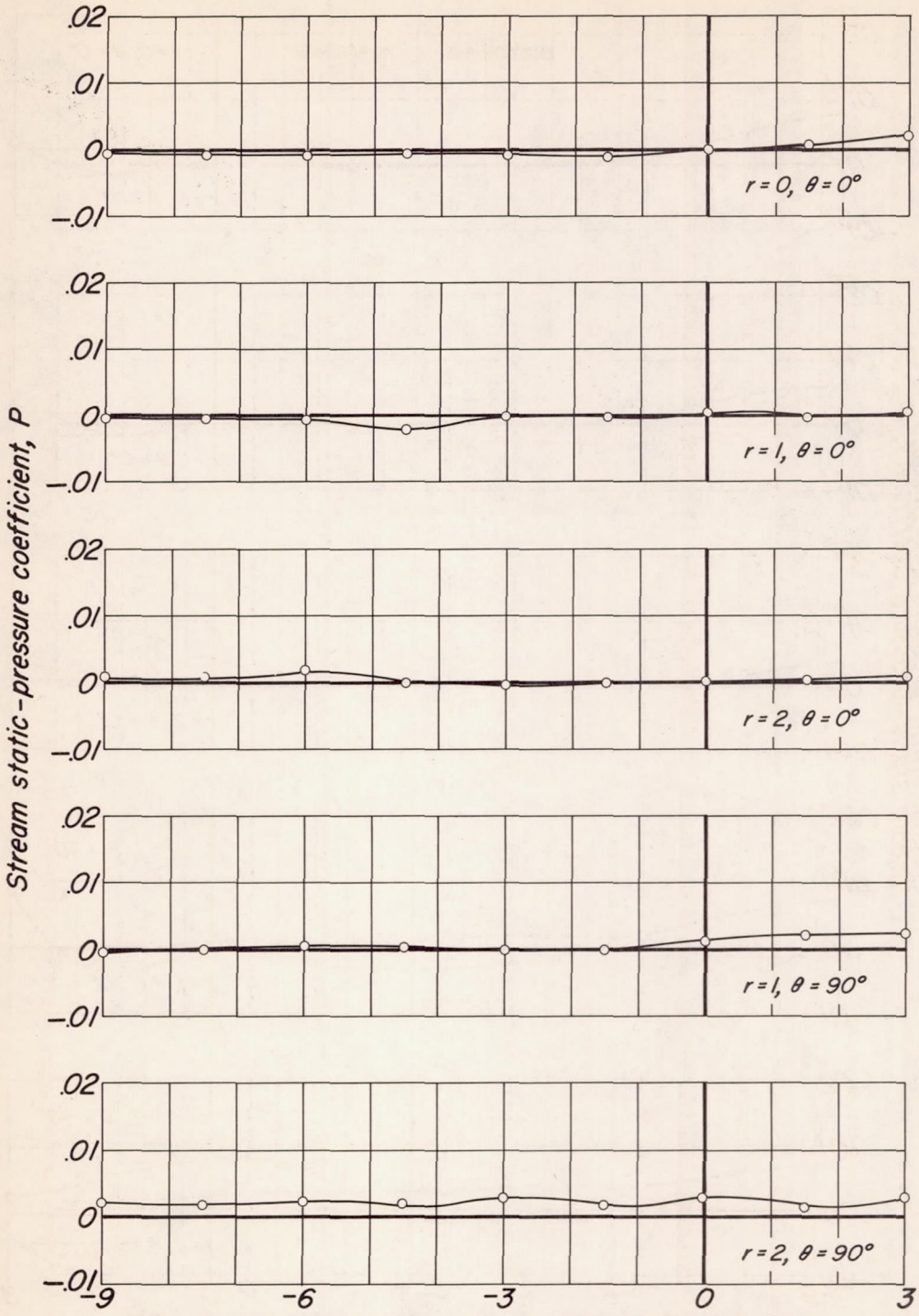

(e) $M = 5.0$, $H_0 = 89$ lb/sq in. abs., $T_0 = 195°$ F

Figure 11.– Continued.

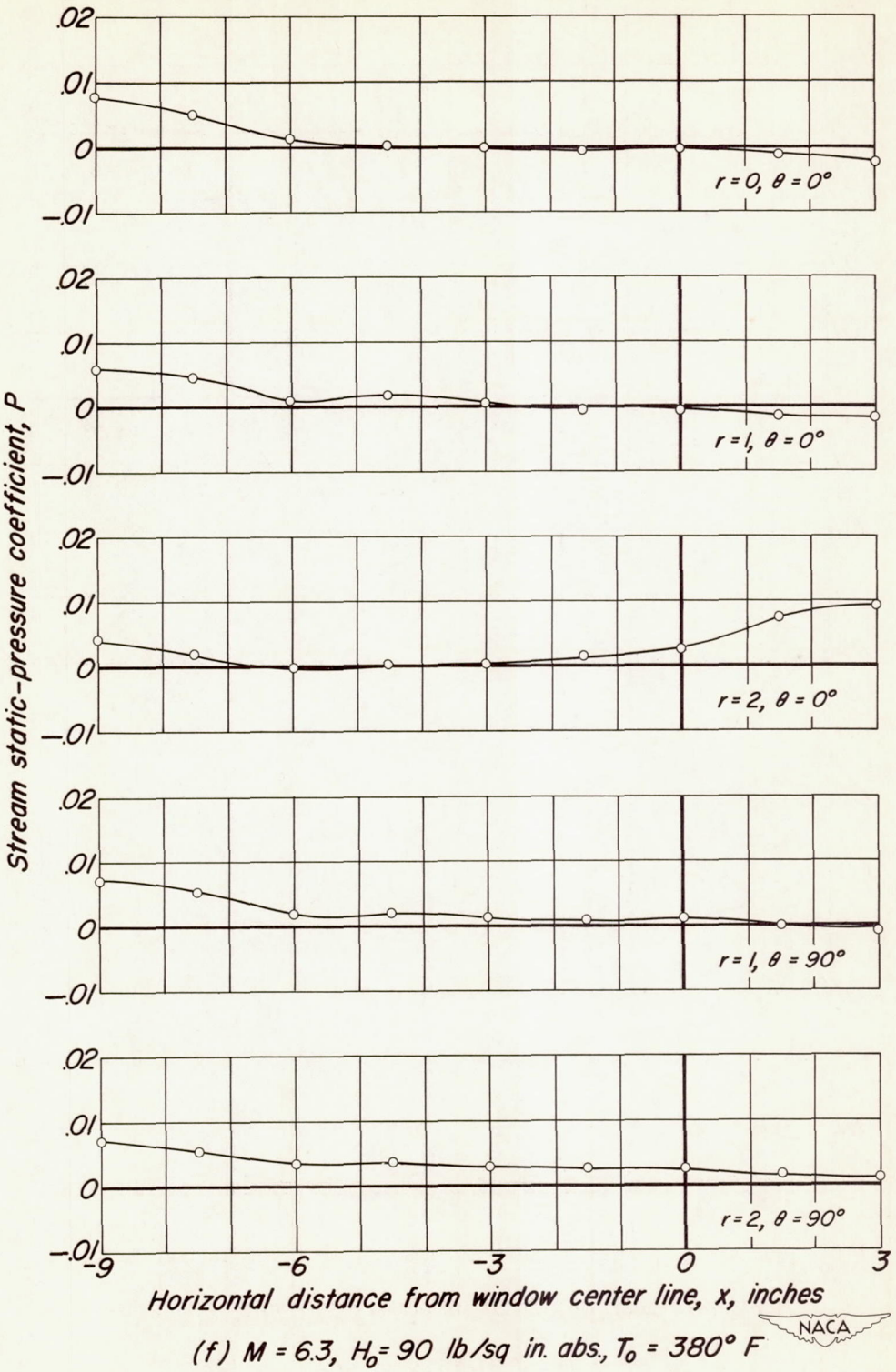

(f) $M = 6.3$, $H_o = 90$ lb/sq in. abs., $T_o = 380°$ F

Figure 11.– Concluded.

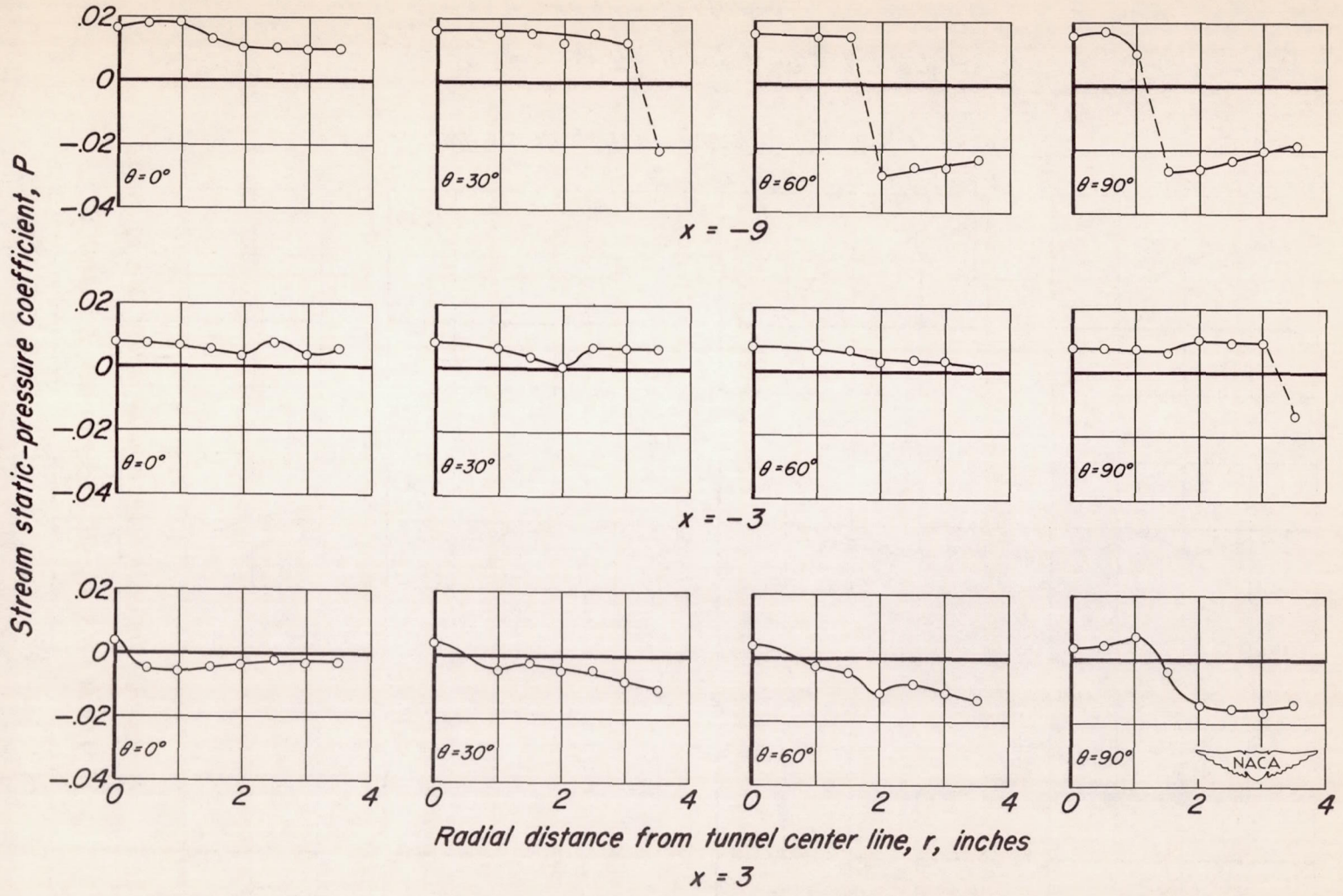

(a) $M = 2.7$, $H_o = 42$ lb/sq in. abs., $T_o = 60°$ F

Figure 12.– Radial variation of stream static-pressure coefficient in the Ames 10- by 14- inch supersonic wind tunnel.

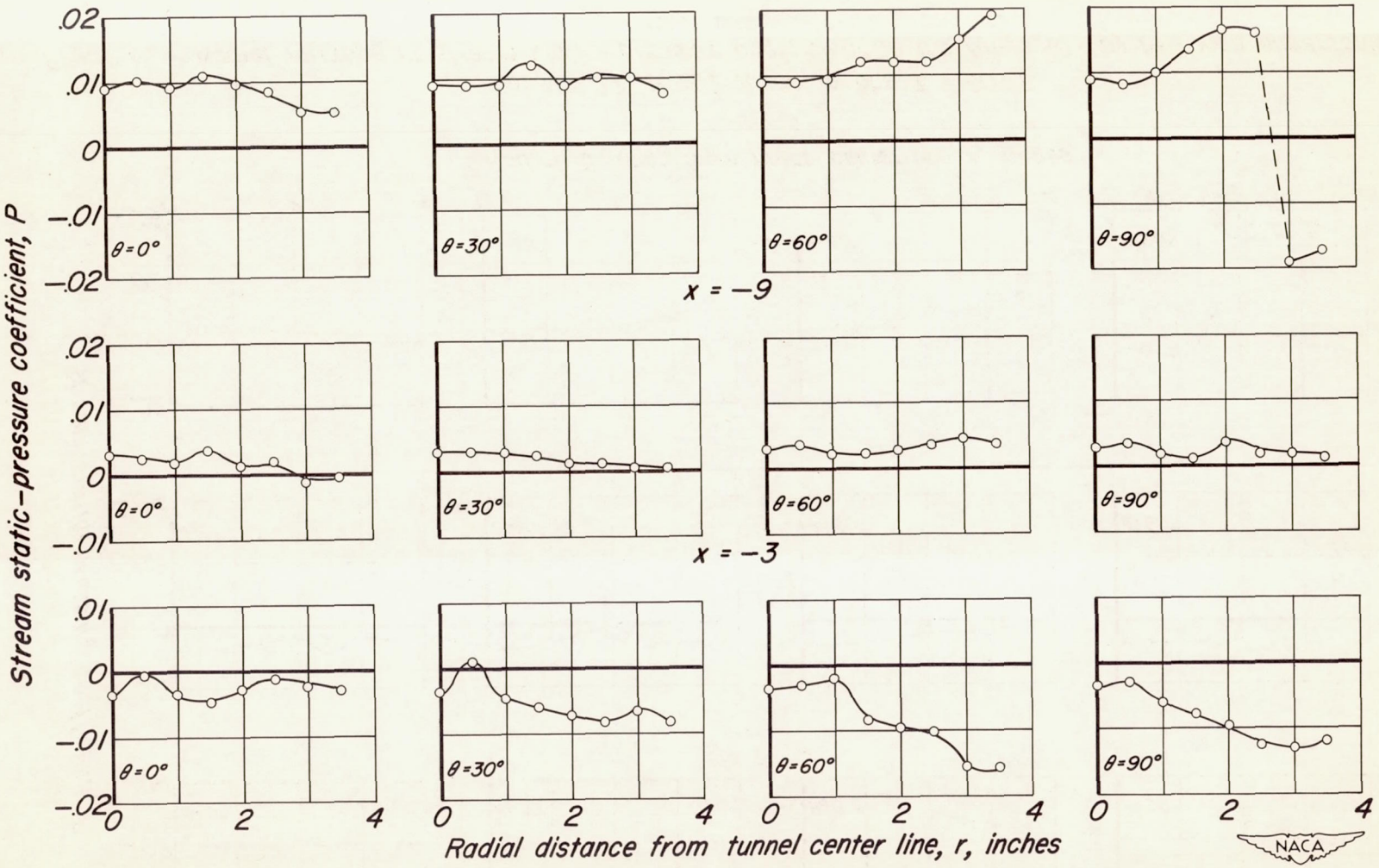

(b) $M = 3.0$, $H_o = 55$ lb/sq in. abs., $T_o = 60°$ F

Figure 12.– Continued.

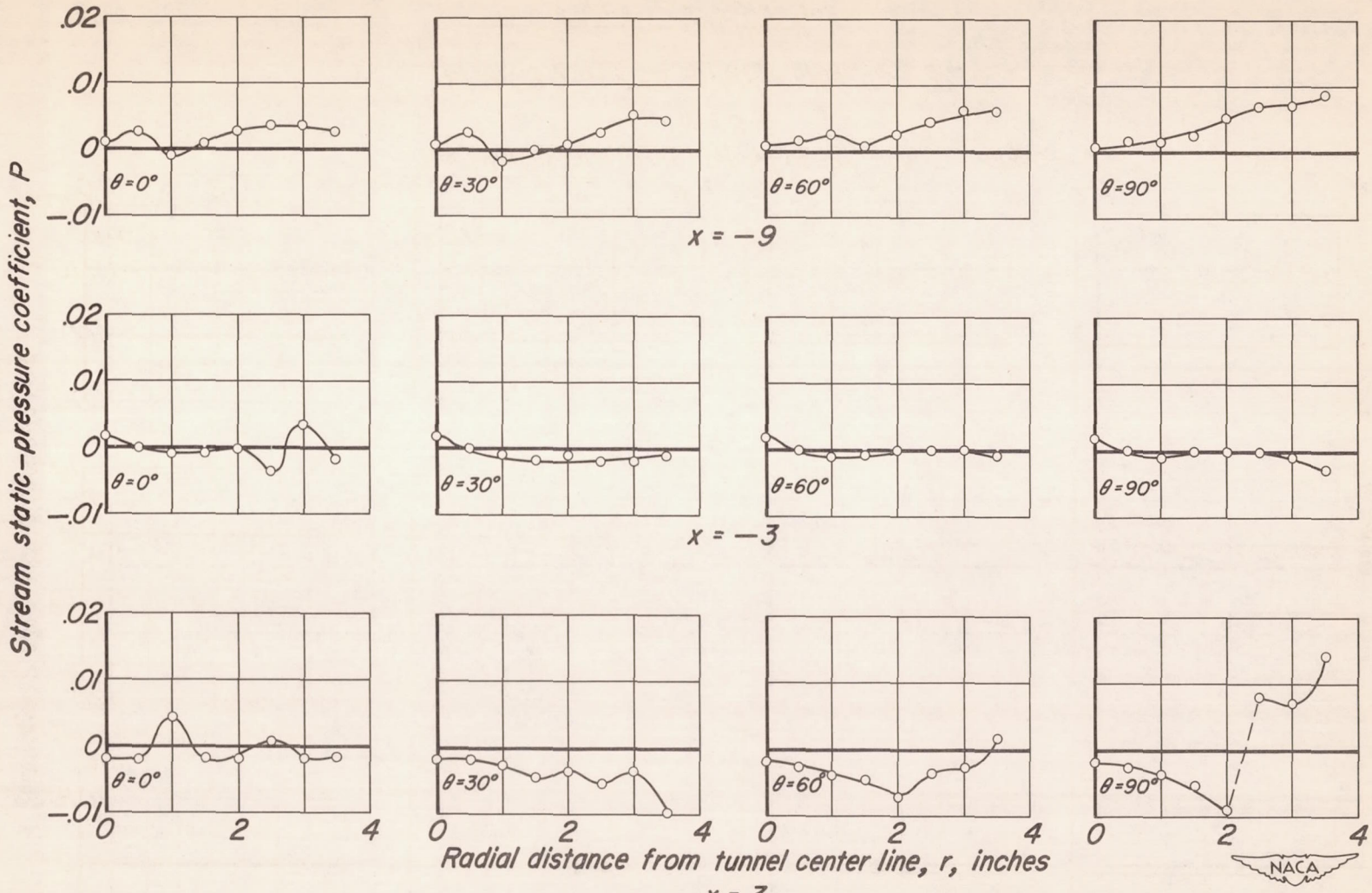

(c) M = 3.5, H_0 = 82 lb/sq in. abs., T_0 = 60° F

Figure 12.– Continued.

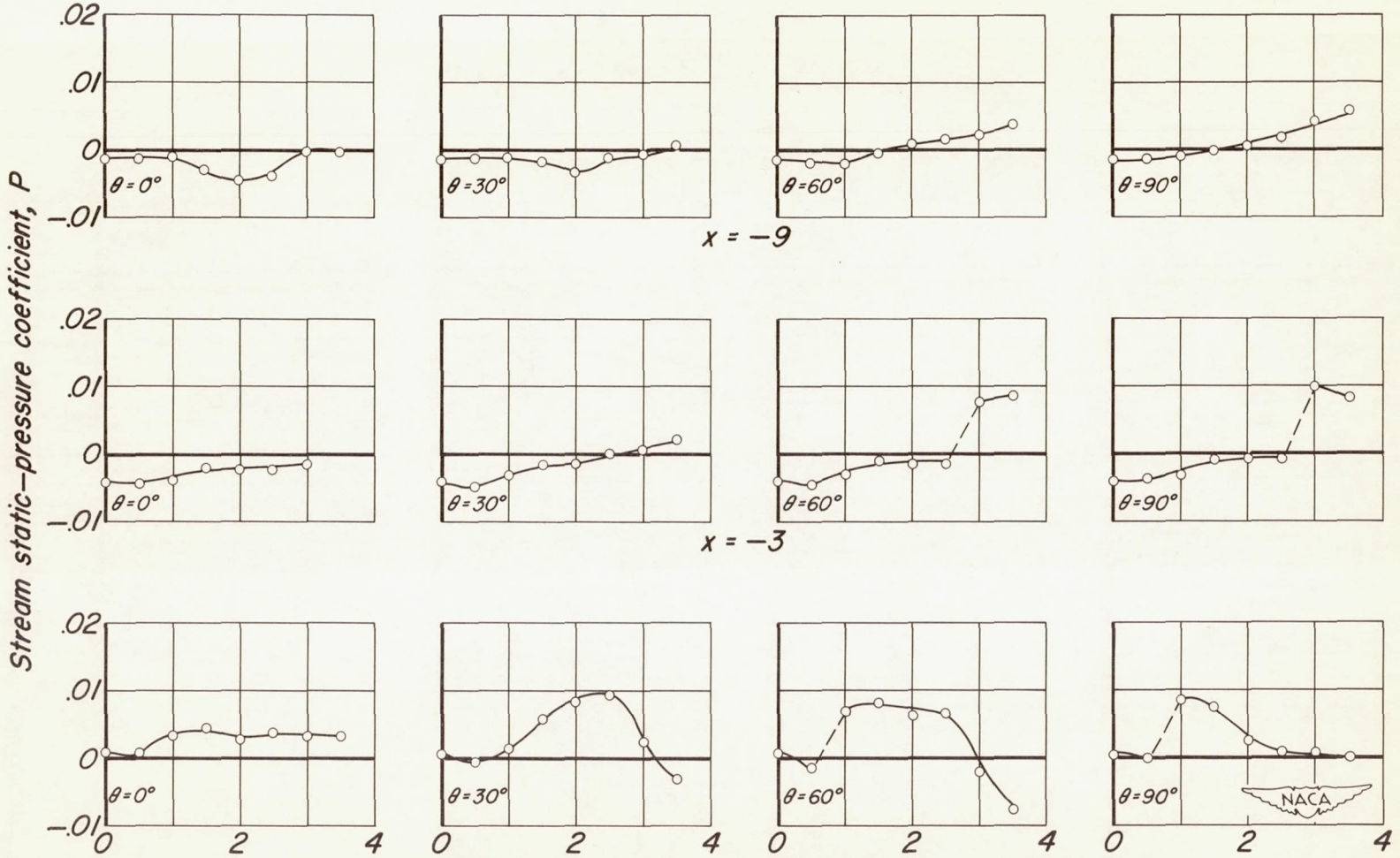

(d) $M = 4.2$, $H_o = 88$ lb/sq in. abs., $T_o = 60°$ F

Figure 12.– Continued.

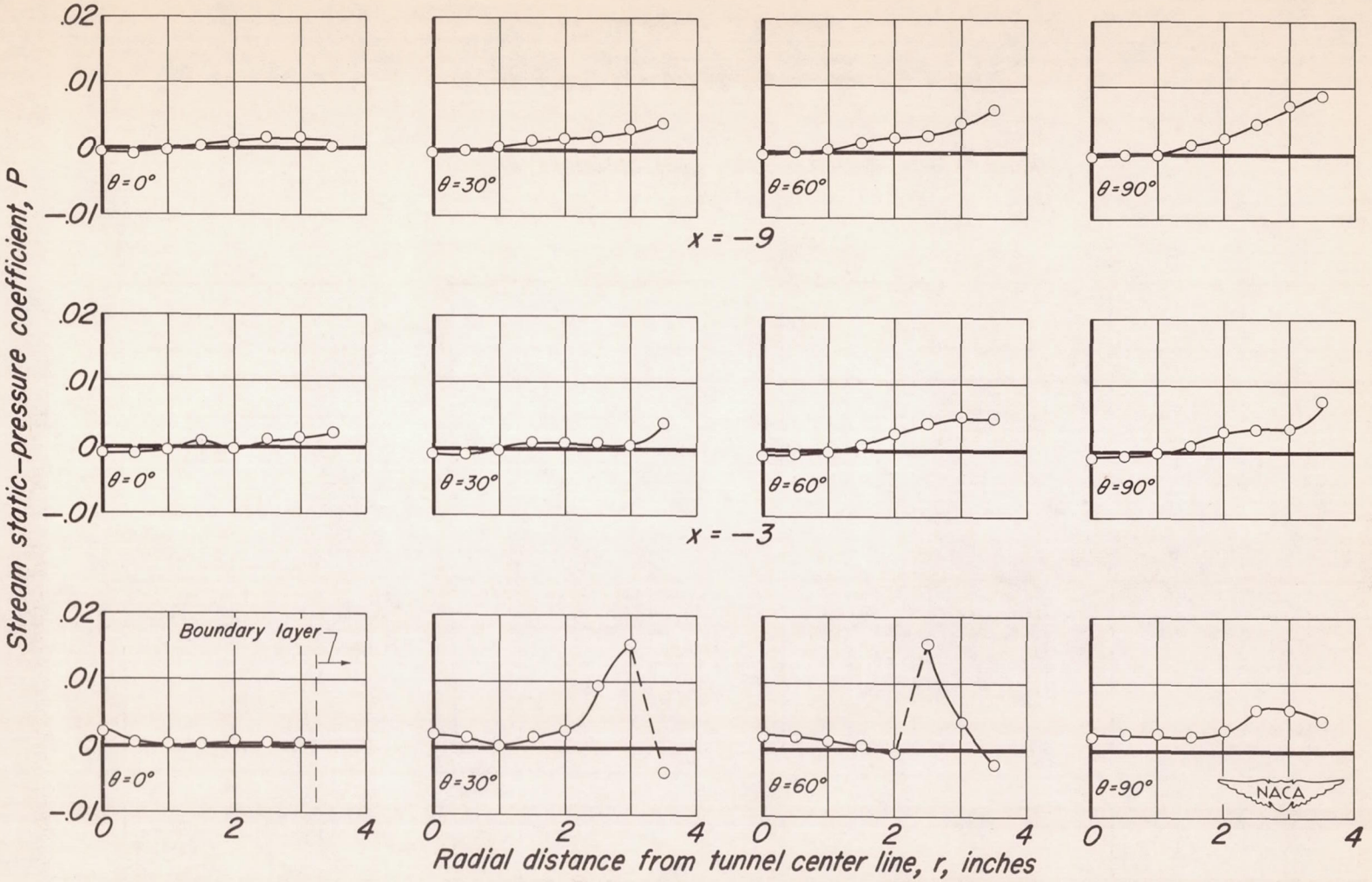

(e) $M = 5.0$, $H_0 = 89$ lb/sq in. abs., $T_0 = 195°$ F

Figure 12.– Continued.

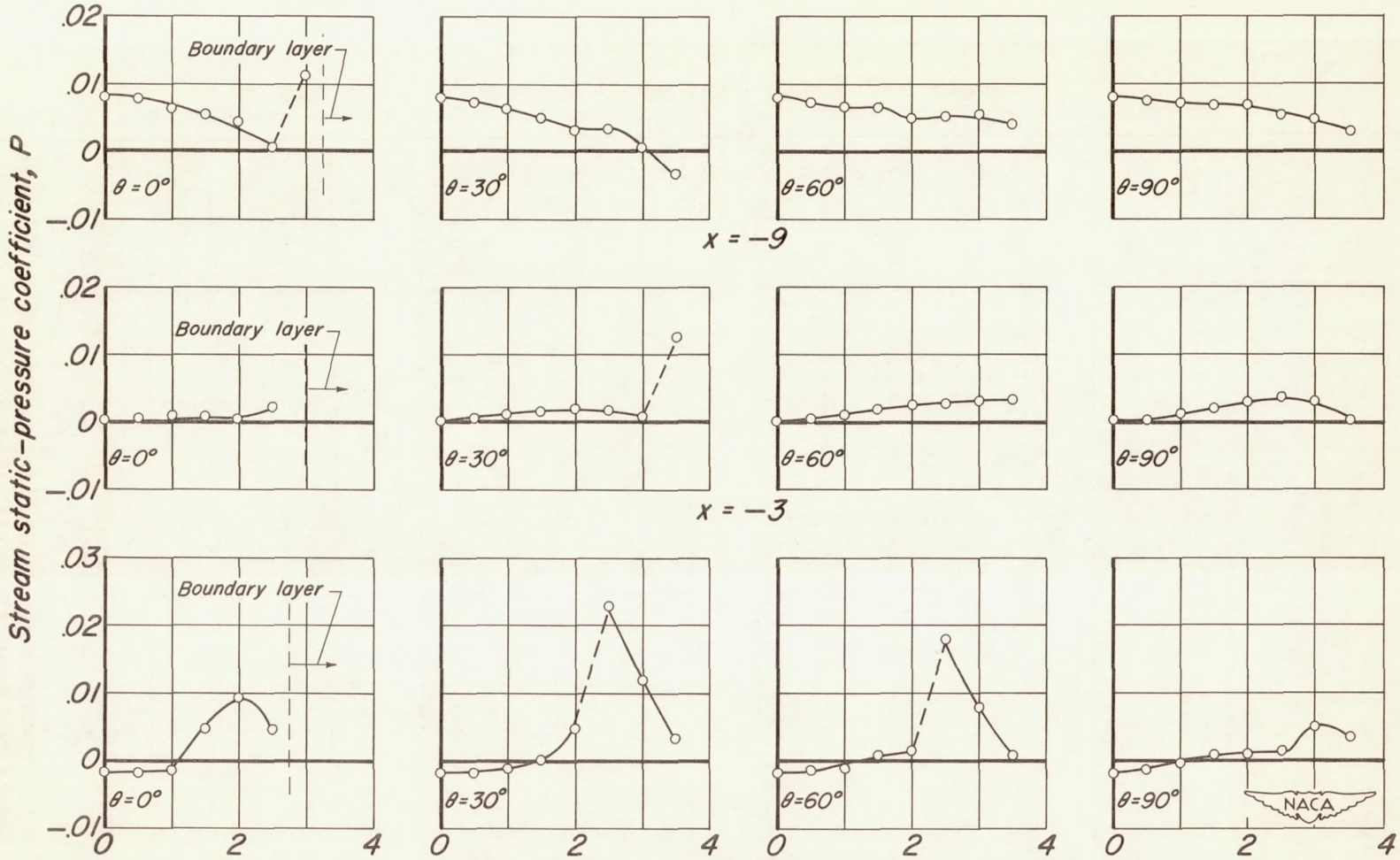

(f) $M = 6.3$, $H_0 = 90$ lb/sq in. abs., $T_0 = 380°$ F

Figure 12.– Concluded.

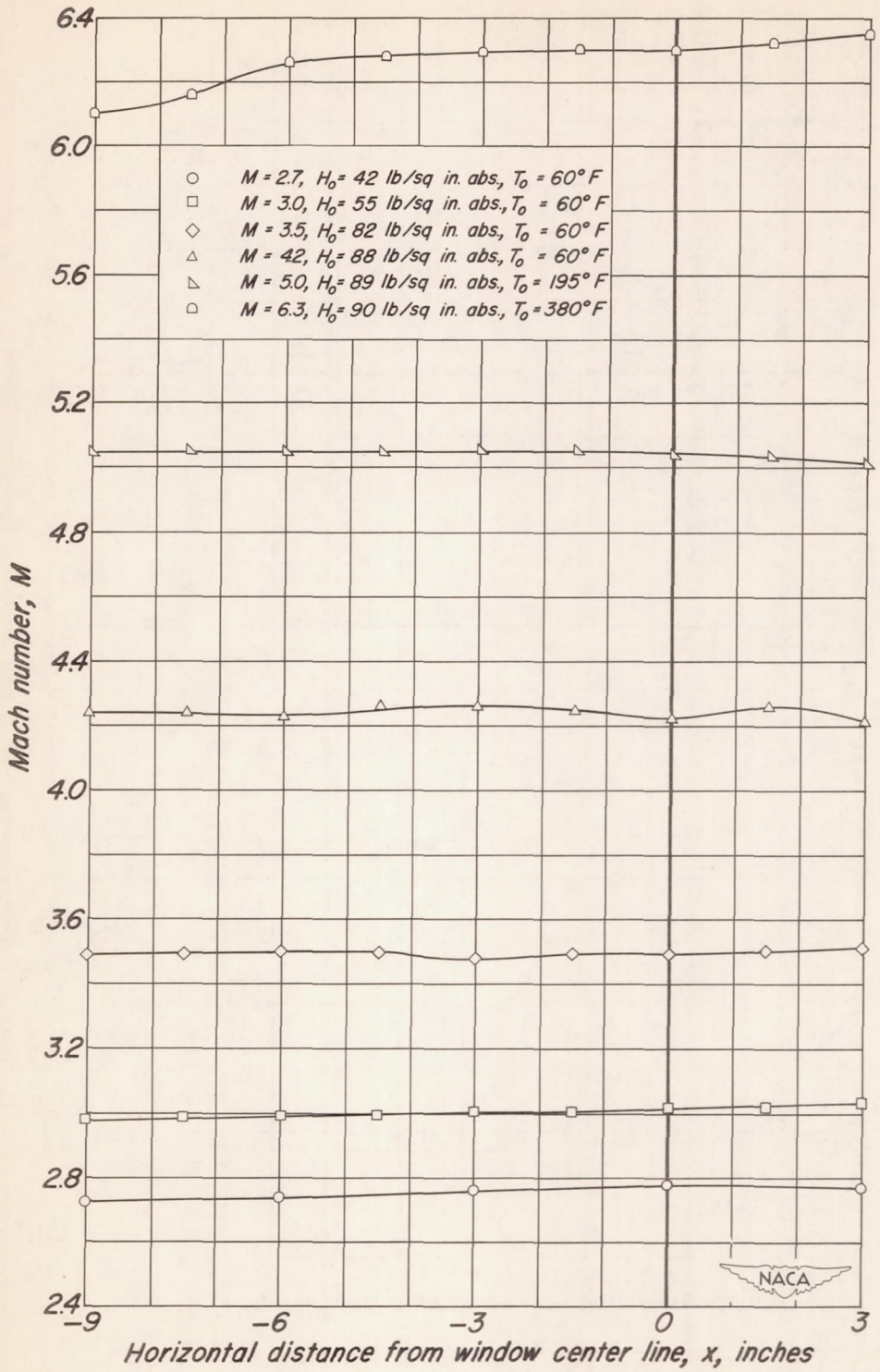

Figure 13.— Longitudinal variation of Mach number along the tunnel center line of the Ames 10- by 14- inch supersonic wind tunnel.

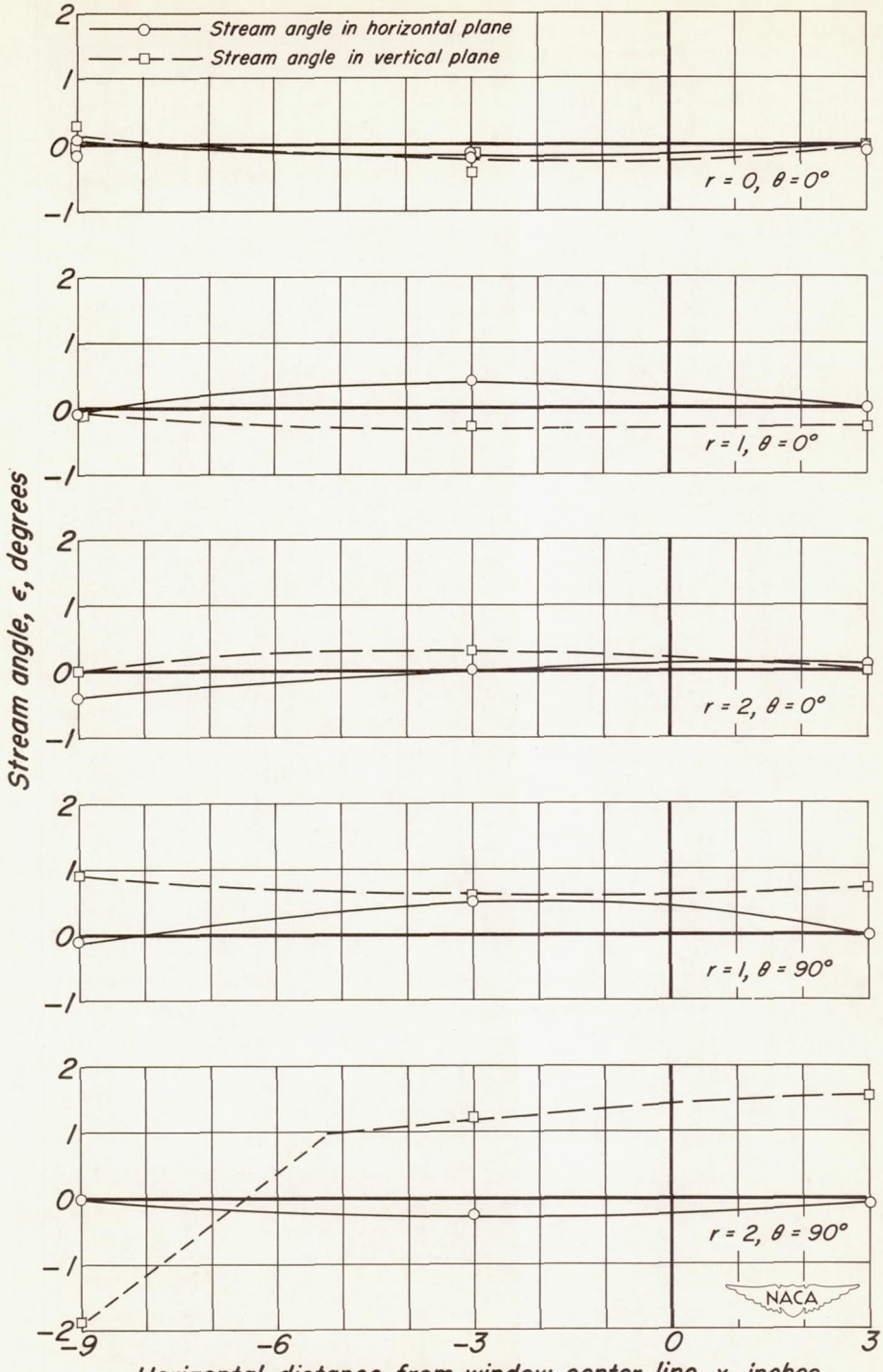

(a) $M = 2.7$, $H_0 = 42$ lb/sq in. abs., $T_0 = 60°$ F

Figure 14.– Longitudinal variation of stream angle in the Ames 10- by 14- inch supersonic wind tunnel.

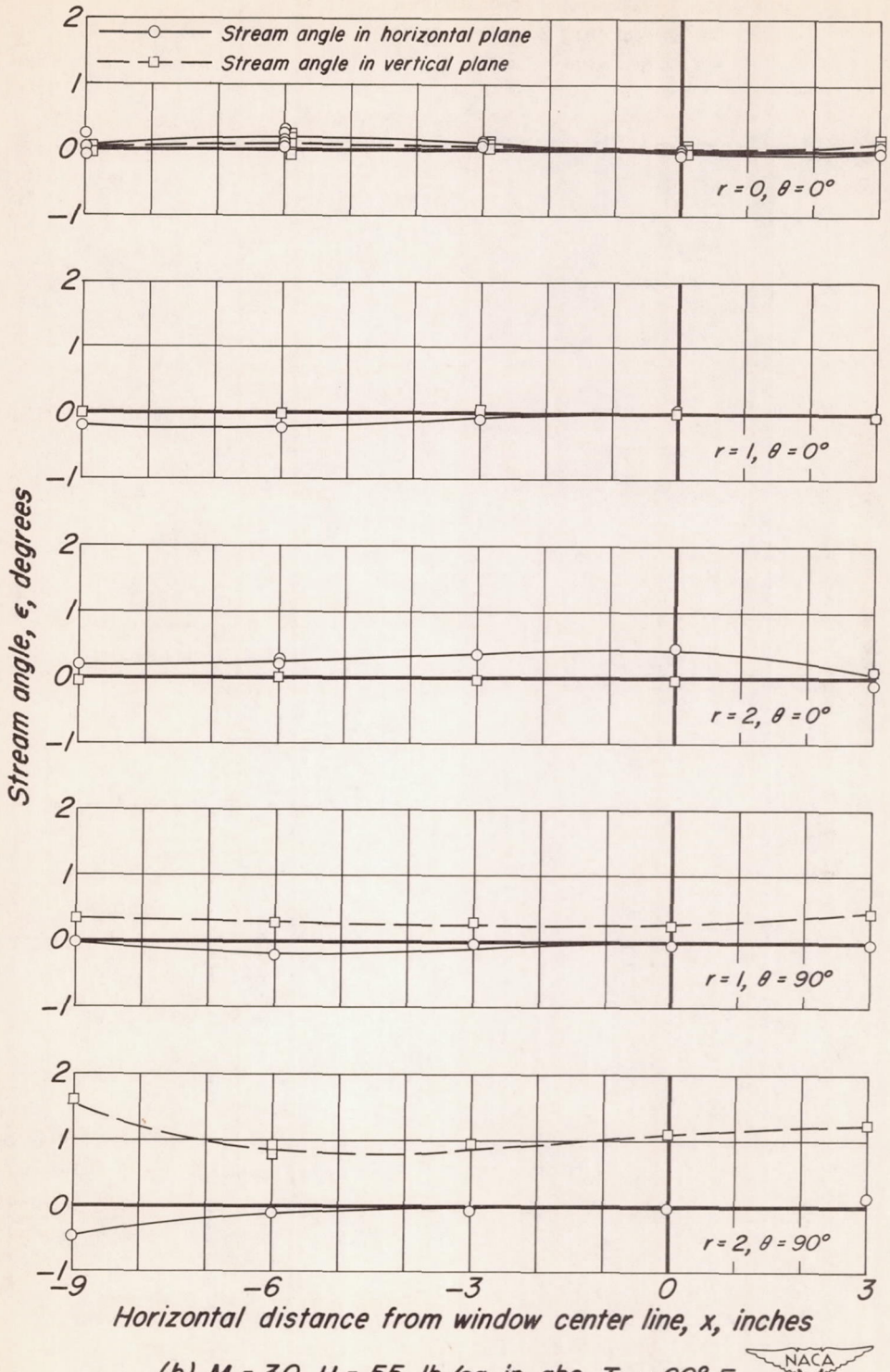

(b) $M = 3.0$, $H_o = 55$ lb/sq in. abs., $T_o = 60°$ F

Figure 14.– Continued.

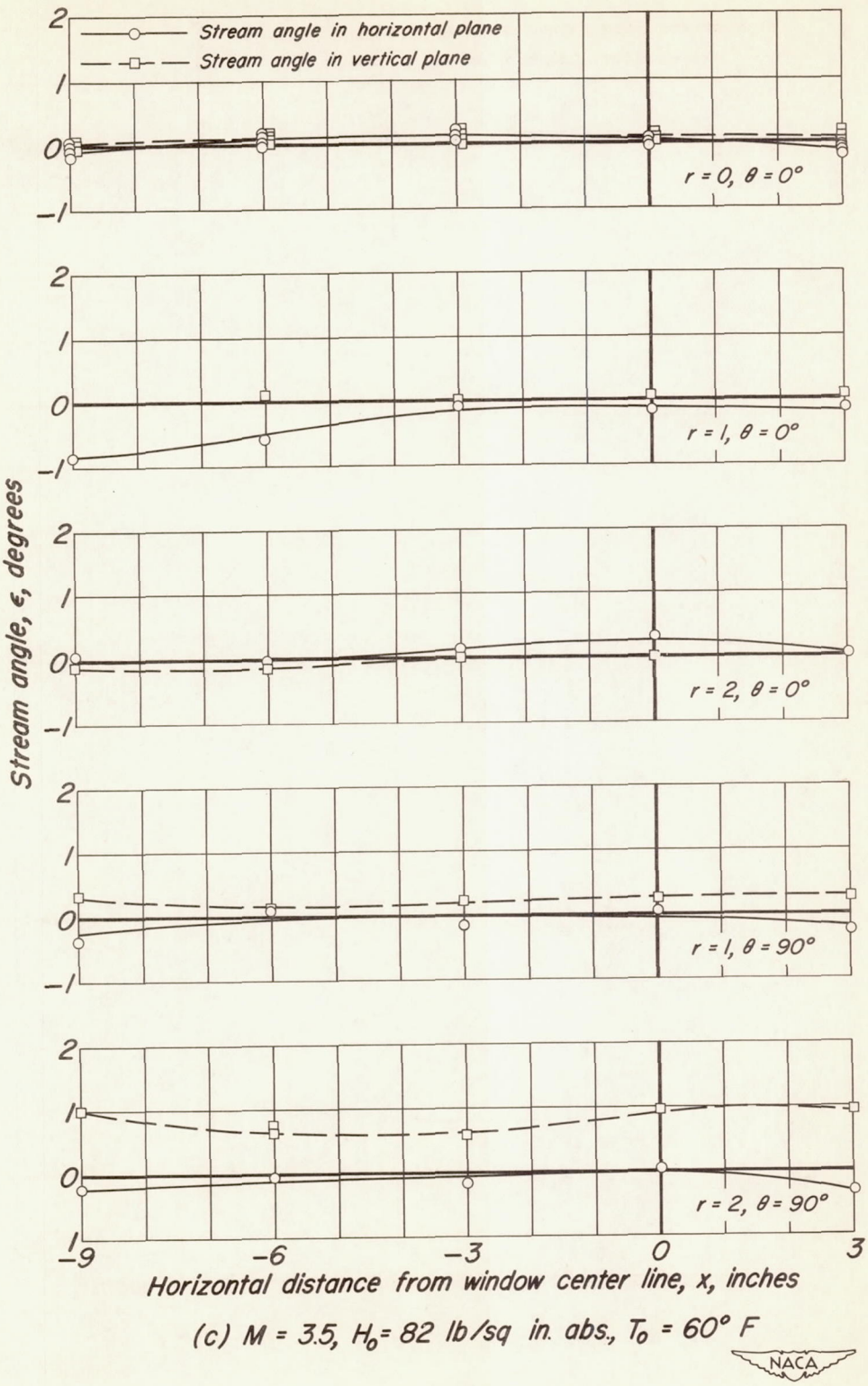

(c) $M = 3.5$, $H_o = 82$ lb/sq in. abs., $T_o = 60°$ F

Figure 14.– Continued.

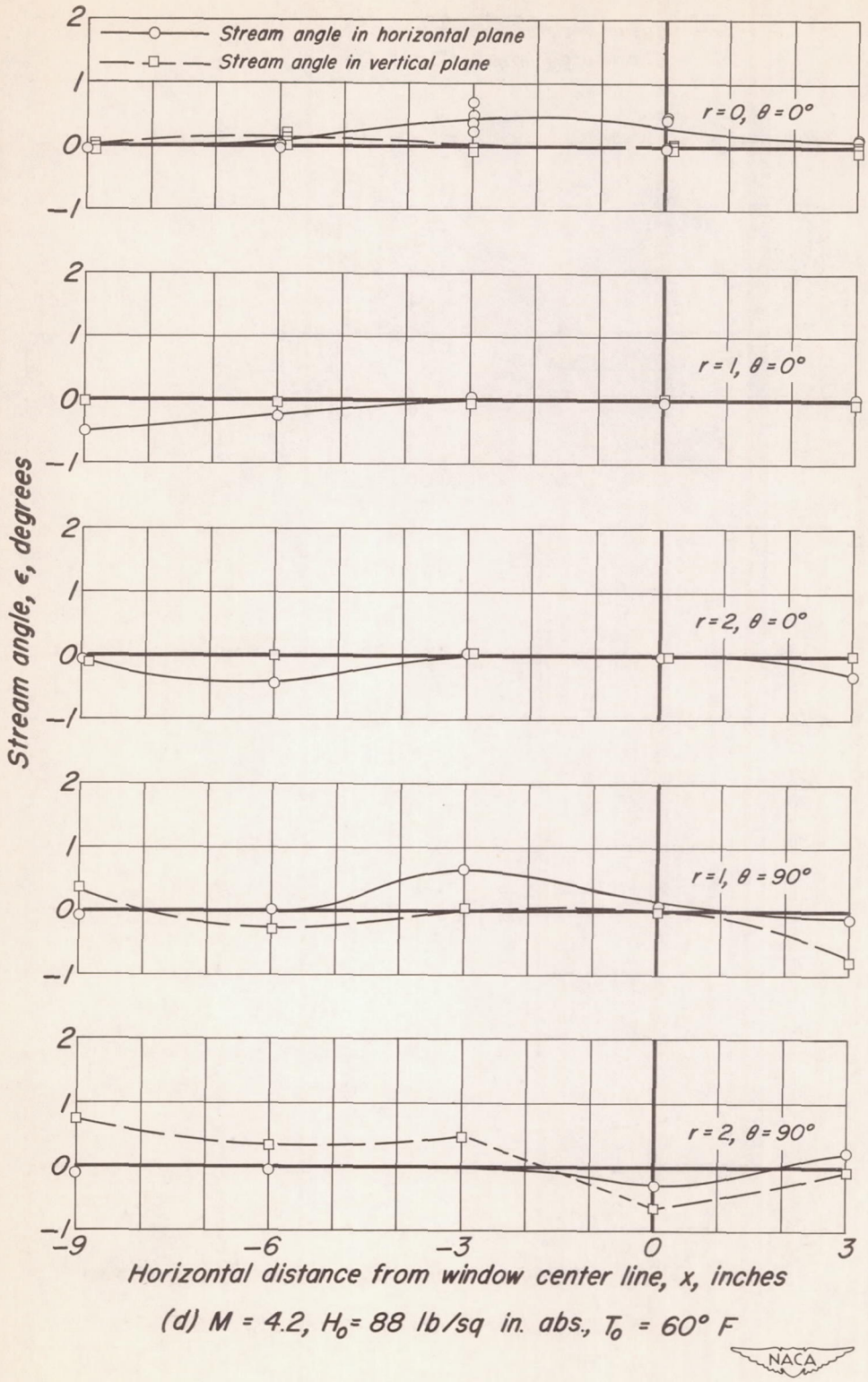

(d) $M = 4.2$, $H_0 = 88$ lb/sq in. abs., $T_0 = 60°$ F

Figure 14.– Continued.

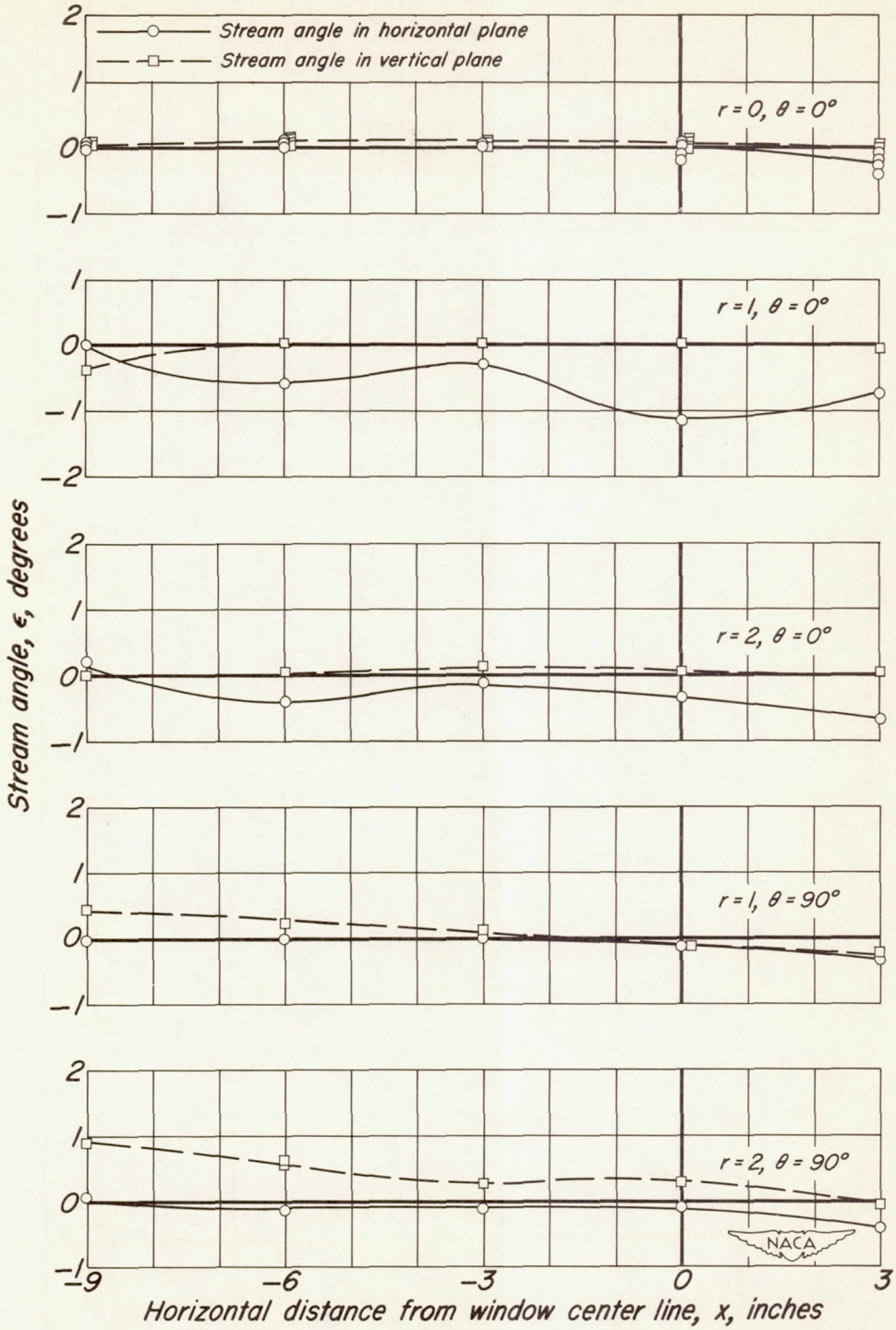

(e) $M = 5.0$, $H_0 = 89$ lb/sq in. abs., $T_0 = 195°$ F

Figure 14.– Continued.

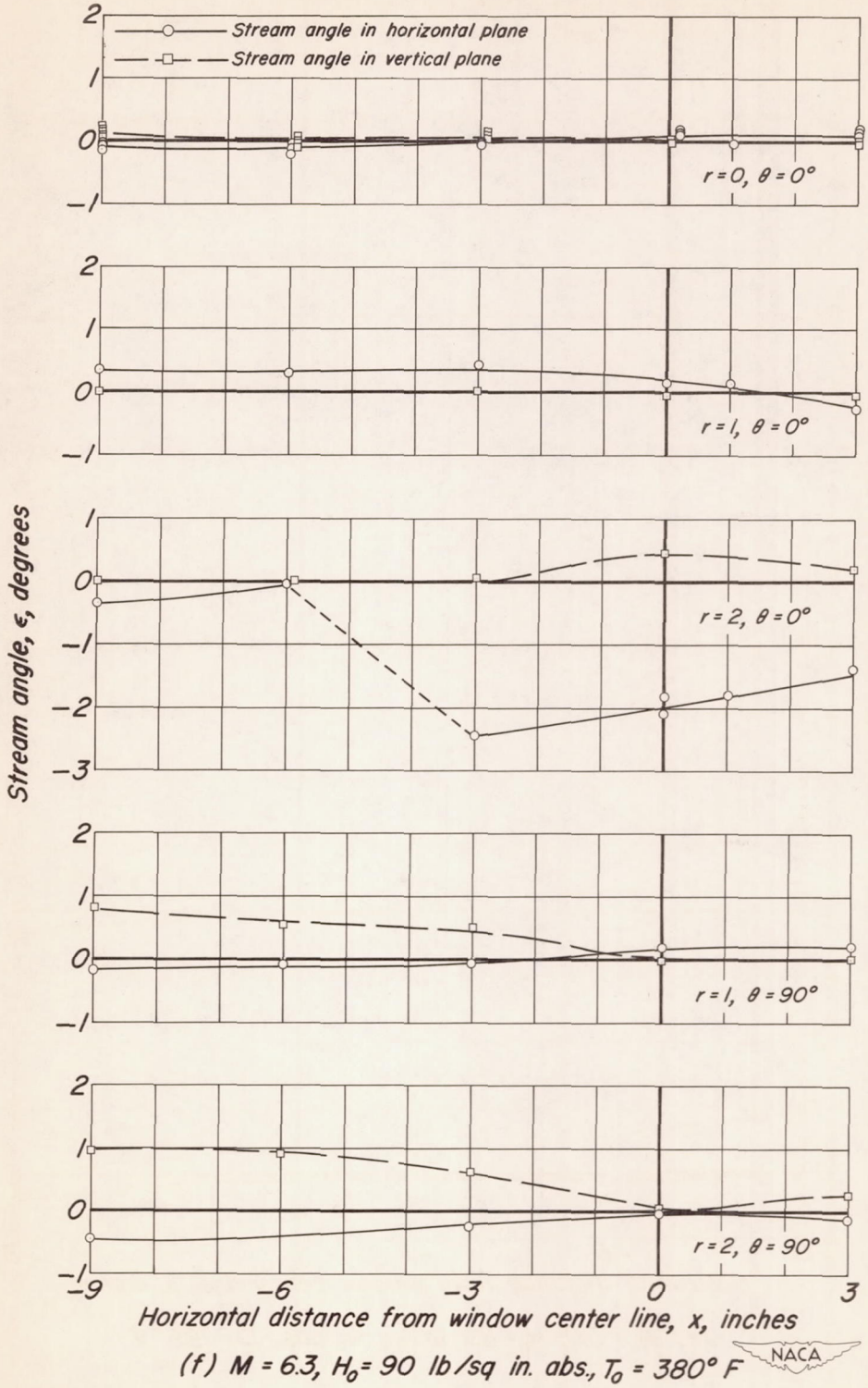

(f) $M = 6.3$, $H_0 = 90$ lb/sq in. abs., $T_0 = 380°$ F

Figure 14.— Concluded.